Splicing Factor 2-Associated Protein p32 Participates in Ribosome Biogenesis by Regulating the Binding of Nop52 and Fibrillarin to Preribosome Particles*[S]

Harunori Yoshikawa,[a] Wataru Komatsu,[b,c,d] Toshiya Hayano,[b,c,e] Yutaka Miura,[a,b,f] Keiichi Homma,[g] Keiichi Izumikawa,[b,f] Hideaki Ishikawa,[b,f] Naoki Miyazawa,[a] Hiroyuki Tachikawa,[b,h] Yoshio Yamauchi,[i] Toshiaki Isobe,[c,f,i] and Nobuhiro Takahashi[a,b,c,f]

Ribosome biogenesis starts with transcription of the large ribosomal RNA precursor (47S pre-rRNA), which soon combines with numerous factors to form the 90S preribosome in the nucleolus. Although the subsequent separation of the pre-90S particle into pre-40S and pre-60S particles is critical for the production process of mature small and large ribosomal subunits, its molecular mechanisms remain undetermined. Here, we present evidence that p32, fibrillarin (FBL), and Nop52 play key roles in this separation step. Mass-based analyses combined with immunoblotting showed that p32 associated with 155 proteins including 31 rRNA-processing factors (of which nine were components of small subunit processome, and six were those of RIX1 complex), 13 chromatin remodeling components, and six general transcription factors required for RNA polymerase III-mediated transcription. Of these, a late rRNA-processing factor Nop52 interacted directly with p32. Immunocytochemical analyses demonstrated that p32 colocalized with an early rRNA-processing factor FBL or Nop52 in the nucleolus and Cajal bodies, but was excluded from the nucleolus after actinomycin D treatment. p32 was present in the pre-ribosomal fractions prepared by cell fractionation or separated by ultracentrifugation of the nuclear extract. p32 also associated with pre-rRNAs including 47S/45S and 32S pre-rRNAs. Furthermore, knockdown of p32 with a small interfering RNA slowed the early processing from 47S/45S pre-rRNAs to 18S rRNA and 32S pre-rRNA. Finally, Nop52 was found to compete with FBL for binding to p32 probably in the nucleolus. Given the fact that FBL and Nop52 are associated with pre-ribosome particles distinctly different from each other, we suggest that p32 is a new rRNA maturation factor involved in the remodeling from pre-90S particles to pre-40S and pre-60S particles that requires the exchange of FBL for Nop52. ***Molecular & Cellular Proteomics 10: 10.1074/mcp.M110.006148, 1–23, 2011.***

From the [a]Department of Applied Life Science, United Graduate School of Agriculture, Tokyo University of Agriculture and Technology, 3-5-8 Saiwai-cho, Fuchu-shi, Tokyo 183-8509, Japan; [b]Department of Applied Life Science, Graduate School of Agriculture, Tokyo University of Agriculture and Technology; [c]Integrated Proteomics System Project, Pioneer Research on Genome the Frontier, Ministry of Education, Culture, Sports, Science and Technology of Japan; [d]Present address: Department of Public Health, Dokkyo Medical University School of Medicine, 880 Kitakobayashi, Mibu, Tochigi 321-0293, Japan; [e]Present address: Department of Biomedical Sciences, College of Life Sciences, Ritsumeikan University, 1-1-1 Nojihigashi, Kusatsu 525-8577, Japan; [f]Core Research for Evolutional Science and Technology (CREST), Japan Science and Technology Agency (JST), Sanbancho 5, Chiyoda-ku, Tokyo 102-0075, Japan; [g]Center for Information Biology-DNA Data Bank of Japan, National Institute of Genetics, Research Organization of Information and Systems, Mishima, Shizuoka 411-8540, Japan; [h]Present address: Graduate School of Agricultural and Life Sciences, University of Tokyo, Japan; [i]Department of Chemistry, Graduate School of Sciences and Engineering, Tokyo Metropolitan University, 1-1 Minamiosawa, Hachioujishi, Tokyo 192-0397, Japan

Received November 4, 2010, and in revised form, April 28, 2011
Published, MCP Papers in Press, May 2, 2011, DOI 10.1074/mcp.M110.006148

Human p32 (splicing factor 2-associated protein p32)[1] contains 282 amino acid residues, 73 of which are in the N-terminal mitochondrial signal sequence. It associates with splicing factor ASF/SF2 (1) and regulates pre-mRNA splicing through its ability to inhibit both phosphorylation and binding of ASF/SF2 to pre-mRNA (2). p32 is also believed to be involved in alternative splicing events by regulating competitive binding of ASF/SF2 and heterogeneous nuclear ribonucleoprotein (hnRNP) A1 to the splicing complex (3–9). p32 has also been identified as a protein (C1QBP) that binds to complement component 1, q subcomponent, which recognizes

[1] The abbreviations used are: p32, splicing factor 2–associated protein p32; FBL, fibrillarin; PRMT, protein arginine methyltransferase; HIV, human immunodeficiency virus; GAR, glycine- and arginine-rich; RBD, RNA-binding domain; hnRNP, heterogeneous nuclear ribonucleoprotein; MW, molecular weight; MS/MS, tandem mass spectrometer; pre-rRNP, preribosomal ribonucleoprotein; siRNA, small interfering RNA; NLS, nuclear localization signal.

and binds to the heavy chain of immunoglobulin G or M initiating the classical complement pathway (10), and as hyaluronic acid-binding protein, which is an inhibitor of *Streptococcus pneumoniae* hyaluronidase (11, 12). p32 also interacts with B subunit of the CCAAT-binding factor and inhibits specifically CCAAT-binding factor-mediated transcription activation (13). In addition, p32 binds the tumor suppressor ARF C terminus, is required for alternative reading frame protein (ARF) to localize to mitochondria, and induces apoptosis (14). Cancer-derived point mutations in the ARF C terminus disrupt simultaneously the ARF-p32 interaction and ARF's apoptotic function; thus, p32 is a critical mediator of ARF's apoptotic function in the mitochondria. p32 links the BH3-only protein Hrk to mitochondria and may be critically involved also in the regulation of Hrk-mediated apoptosis (15). So far, a dozen other intracellular proteins, including the lamin B receptor (16), mitogen-activated protein kinases, protein kinase C family proteins, and matrix metallopeptidase, have been found to associate with p32 (NCBI Entrez Gene, C1QBP). Furthermore, it interacts with several viral proteins, including herpes simplex virus 1 Orf-P protein (17), the adenovirus polypeptide V (18), Epstein-Barr virus EBNA 1 protein (19, 20), rubella virus capsid protein (21), and the human immunodeficiency virus 1 (HIV1) Rev (22, 23) and Tat proteins (24). Although most of the physiological functions of these interactions are not understood, p32 was found to inhibit the splicing of HIV pre-RNA transcripts in HIV-transfected cells (25). A single mutation in human p32 of Gly35 to Asp35, which is also found in murine p32, abrogates this effect. HIV uses the splicing inhibition function of human p32, but not of the mouse counterpart, in RNA splicing to escape from a mechanism underlying the host cell defense against viral infection.

Although p32 is predominantly localized in mitochondria and on the cell surface, we previously found that it interacts with a nucleolar protein, fibrillarin (FBL), in a subcomplex containing a minimal set of proteins including protein arginine methyltransferase 5 (PRMT5, Janus Kinase-binding protein 1), and PRMT1 (26). FBL is the most abundant protein in the dense fibrillar regions of the nucleolus where rRNA transcription and early pre-rRNA processing take place (27). FBL is a methyltransferase and a component of RNP complexes (small subunit prosessome) that contain U3, U8, U13, and other small nucleolar RNAs. FBL associates with Nop56, Nop5/58 and a 15.5-kDa protein (a counterpart of yeast Snu13p) to form box C/D snoRNP complexes that function in site-specific 2′-*O*-methylation of RNA (28–31), and is a component of the pre-90S ribosomal particle formed at the early stages of ribosome biogenesis in the nucleolus. Human FBL (~36 kDa) comprises glycine- and arginine-rich (GAR) domain, RNA-binding domain (RBD) and methyltransferase-like domain (32). Both the FBL GAR domain and the subsequent spacer region 1 (residues 78–132) interact directly with p32 (26).

In this study, we performed a proteomic analysis of protein complexes pulled down from nuclear extract with p32 as bait and found that it associated with many probable rRNA processing factors. Among them, p32 was found to interact with Nop52 (NNP1/RRP1A) without any cofactors, as does it FBL. Nop52 is a human homolog of yeast Rrp1p, which is associated with several distinct 66S pre-ribosomal particles in yeast cells and is involved in late events related to the production of 60S ribosomal subunit (33). Nop52, which was originally identified with human autoantibodies, is a nucleolar protein that is excluded from rRNA transcription sites, accumulates in the granular external domain, and mainly co-localizes with nucleolar proteins such as B23 that are involved in the late processing step in the nucleoli (34, 35). The perinucleolar bodies sequentially recruit FBL, nucleolin, and Nop52 together with protein B23, in this order, during the formation of the nucleolus at the end of mitosis (34, 35). Our present study demonstrates that p32 is required for processing of pre-rRNAs at the early nucleolar stages of ribosome biogenesis.

EXPERIMENTAL PROCEDURES

Construction of Epitope-tagged Expression Plasmids—Reverse transcriptase (RT)-PCR was performed with the Super Script II kit (Invitrogen) according to the manufacturer's instructions using total mRNA that was prepared from 293EBNA cells (Invitrogen). C-terminally FLAG (DYKDDDDK)-tagged p32 (p32-FLAG) cDNA, C-terminally FLAG-tagged Guα (FLAG-Guα) cDNA, and N-terminally FLAG-tagged Guβ (FLAG-Guβ) cDNA were amplified by PCR using the primer sets 5′-ATTGAGCTAGCGCCACCATGCTGCCTCTGCTGCGCTGC-3′ and 5′-TCAGTGGATCCCTACTTGTCGTCGTCGTCCTTGTAGTCCTGGCTCTTGACAAAACTCTT-3′ for p32-FLAG, 5′-ATATAGCTAGCGCCACCATGCCGGGAAAACTCCGTAGTGACGCTGGT-3′ and 5′-ATATAGGATCCTTACTTGTCGTCGTCGTCCTTGTAGTCTTGACCAAATGCTTTACTGAAACTCCGCTT-3′ for FLAG-Guα, and 5′-TATAATGGATCCGCCACCATGGACTACAAGGACGACGACGACAAGATGCCTGGGAAACTCCTCTGG-3′ and 5′-CAACTCGAGTCAGTCAAAACTCCGTTTGTG-3′ for FLAG-Guβ. The PCR products were cloned into the NheI/BamHI sites (for p32-FLAG and FLAG-Guα) and into the BamHI/XhoI sites (for FLAG-Guβ) of the expression vector pcDNA3.1(+). Previous reports have described the construction of FLAG-tagged nucleolin (FLAG-NCL) (36), FLAG-tagged FBL (FLAG-FBL) (26), and FLAG-tagged Nop52 (FLAG-Nop52) (37). N-terminally HA (YPYDVPDYA)-tagged FBL (HA-FBL) was amplified from the expression vector containing the FLAG-tagged FBL-coded DNA fragment as the template by PCR using the primer sets 5′GAAGAAGGATCCGCCACCATGTACCCATACGACGTGCCTGACTATGCCAAGCCAGGATTCAGTCCCCGT-3′ and 5′-GAAGAAGAATTCTCAGTTCTTCACCTTGGGGGG-3′. The PCR product was cloned into the BamHI/EcoRI sites of the expression vector pcDNA3.1(+). To establish inducible FLAG-Nop52 expression cell lines, cDNA for FLAG-Nop52 was amplified by PCR using the forward primer 5′ATATCAAGCTTGCCAACCATGGACTACAAGGACGACGACGACAAGGTTTCGCGCGTGCAGCTCCCG-3′ and the reverse primers described previously (37). The PCR product was cloned into the HindIII/BamHI sites of the expression vector pcDNA5/FRT/TO. All constructs were verified by DNA sequencing.

RNA Interference (RNAi)—HeLa cells were cultured in 35-mm dishes until they reached 80% confluency, and transfected with 2.5 μl Lipofectamine 2000 and 50 nM stealth small interfering RNA (siRNA)615. The following stealth siRNA sequences were used: 5′-AUGACAGUCCAACACAAGGGCCUUC-3′ and 5′-GAAGGCCCUUGUGUUGGACUGUCAU-3′ for p32 knockdown and 5′-AUGCCAACUGCCAAACACGAGGUUC-3′ and 5′-GAACCUCGUGUUUGGCAGU-

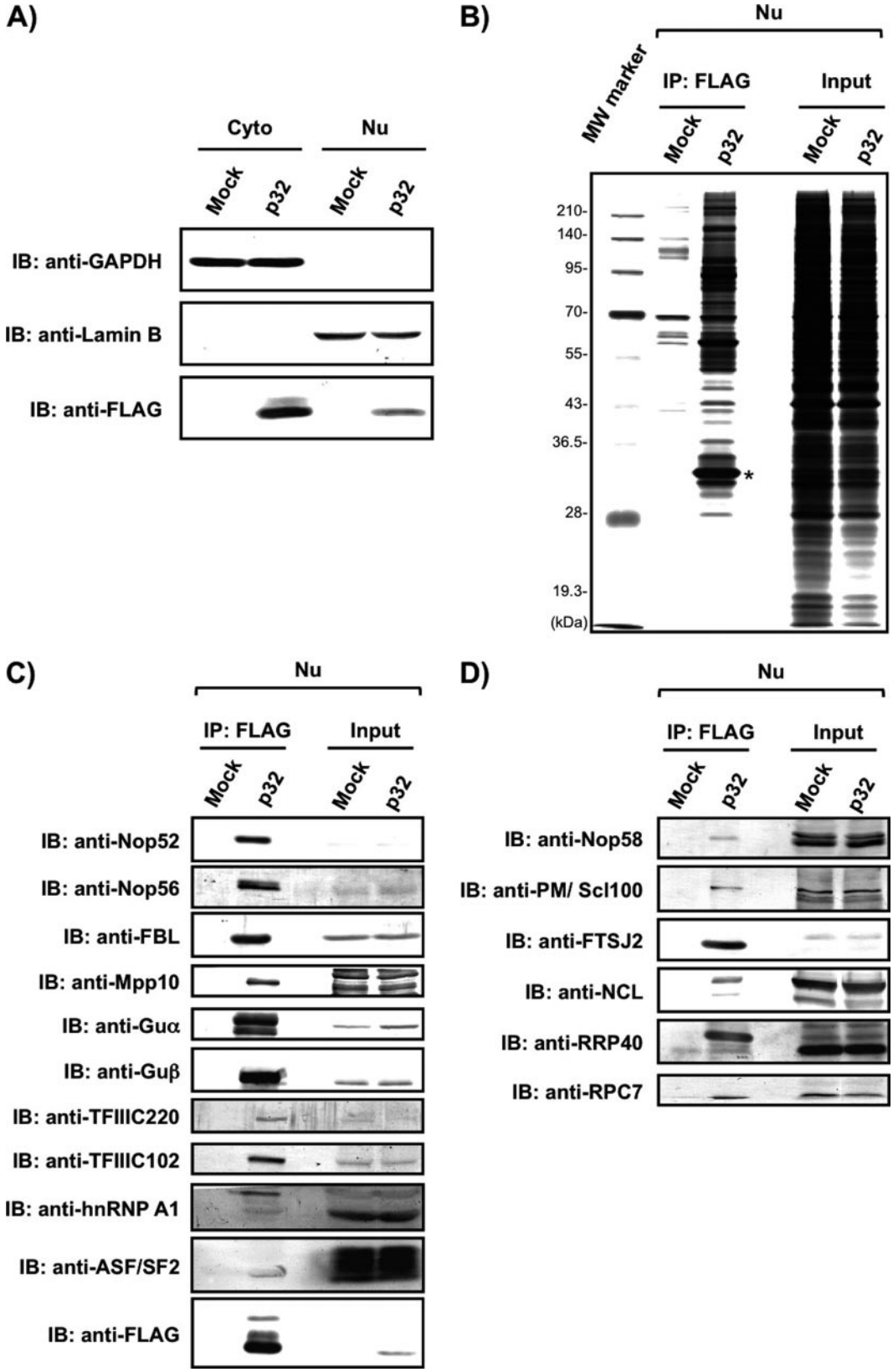
A)
Cyto
Nu
Mock
p32
Mock
p32
IB: anti-GAPDH
IB: anti-Lamin B
IB: anti-FLAG
B)
Nu
MW marker
IP: FLAG
Input
Mock
p32
Mock
p32
210-
140-
95-
70-
55-
43-
36.5-
28-
19.3-
(kDa)
*
C)
Nu
IP: FLAG
Input
Mock
p32
Mock
p32
IB: anti-Nop52
IB: anti-Nop56
IB: anti-FBL
IB: anti-Mpp10
IB: anti-Guα
IB: anti-Guβ
IB: anti-TFIIIC220
IB: anti-TFIIIC102
IB: anti-hnRNP A1
IB: anti-ASF/SF2
IB: anti-FLAG
D)
Nu
IP: FLAG
Input
Mock
p32
Mock
p32
IB: anti-Nop58
IB: anti-PM/ Scl100
IB: anti-FTSJ2
IB: anti-NCL
IB: anti-RRP40
IB: anti-RPC7

UGGCAU-3′ for the negative control. The cells were transferred to 35-mm or 90-mm dishes 24 h after the first transfection and then transfected again with the same stealth siRNA 48 h after the first transfection. The cells were then cultured for 12 h and were washed once with PBS and cultured in Dulbecco's modified Eagle's medium (Invitrogen, Carlsbad, CA) containing 10% FBS, streptomycin (0.1 mg/ml), penicillin G (100 U/ml), and 1000 mg/L glucose for additional 12 h.

Cell Fractionation—Subconfluent p32-FLAG-transfected 293EBNA, inducible FLAG-Nop52 expression (Flp-In T-REx 293) cells, 293EBNA cells, or HeLa cells were collected from four 90-mm dishes, lysed by vortexing for 10 s with 1 ml buffer A (16.7 mM Tris-HCl (pH 8.0), 50 mM NaCl, 1.67 mM $MgCl_2$, 1 mM phenylmethylsulfonyl fluoride (PMSF)) containing 0.1% Triton X-100, incubated for 5 min on ice, and centrifuged at 1,000 × *g* for 5 min. The supernatant was collected as the cytoplasmic fraction. The nuclear extract (Nu), nucleoplasmic extract (NE) and nucleolar/Cajal bodies extract (NoE) were prepared from the remaining pellet as described (38) with the following modifications. To fully remove the cytoplasmic constituents, the pellet was suspended again with 1 ml buffer A and collected by centrifugation (the nuclear pellet). To prepare Nu, the nuclear pellet was sonicated in 500 μl of lysis buffer (50 mM Tris-HCl pH 8.0, 150 mM NaCl, 5 mM $MgCl_2$, and 0.5% IGEPAL CA630) containing 1 mM PMSF and 20 U SUPERase·In (Ambion) three times for 20 s at 4 °C with a Bioruptor (Cosmo Bio) at the highest setting, and centrifuged for 15 min at 15,000 × *g*. The supernatant was used as the Nu. To prepare NE, the nuclear pellet was re-suspended with 500 μl of the lysis buffer, and sonicated ten times for 20 s at 4 °C with a Bioruptor at the highest setting, and then centrifuged for 30 min at 15,000 × *g*. The supernatant was used as the NE. The resulting pellet was resuspended with 500 μl NoE buffer (50 mM Tris-HCl pH 8.0, 150 mM NaCl, 10 mM EDTA, 10 mM dithiothreitol, 1 mM PMSF and 20 U Superasin), and sonicated ten times for 20 s at 4 °C, and then centrifuged for 30 min at 15,000 × *g*. The supernatant was used as the NoE. These extracts were examined for cross-contamination by immunoblot analysis using antibodies against GAPDH as a marker of the cytoplasm, lamin B as a nuclear marker, Nop58 as a nucleolar marker, and p80-coilin as a marker for Cajal bodies.

Immunoprecipitation and Immunoblot Analysis—After transfection for 48 h, FLAG-tagged protein- or FLAG-tagged mutant-transfected 293EBNA cells were harvested from two 90-mm dishes, washed with PBS and lysed by vigorous vortexing for 30 s in 1 ml lysis buffer, and incubated on ice for 30 min (40). The soluble fraction was obtained by centrifugation at 20,000 × *g* for 30 min at 4 °C. At least 5 mg of total cell lysate or the Nu described above was incubated with 10 μl anti-FLAG M2 agarose beads for 2 h at 4 °C. After washing the agarose beads with 1 ml lysis buffer five times and once with 50 mM Tris-HCl pH 8.0, containing 150 mM NaCl and 5 mM $MgCl_2$, the complexes bound to the agarose beads were eluted with 500 μg/ml FLAG peptide. The eluted complexes were separated by SDS-PAGE and electrophoretically transferred to PVDF membranes. The membranes were blocked with 3% nonfat dried skim milk in phosphate-buffered saline (PBS) at 4 °C at least for 1 h, and incubated with the appropriate primary antibody overnight at 4 °C. The membranes were washed three times with PBST (PBS containing 0.1% (w/v) Tween 20) for 10 min, incubated with secondary antibody conjugated with alkaline phosphatase for 1 h at room temperature, washed three times with PBST for 10 min, and washed once with PBS for 5 min. Staining was performed in NBT (nitro-blue tetrazolium chloride)/BCIP (5-bromo-4-chloro-3′-Indolylphosphatase *p*-toluidine salt) solution, prepared by a (1:50) dilution of NBT/BCIP stock solution with alkaline phosphatase buffer (100 mM Tris-HCl pH 9.5, 100 mM NaCl, 50 mM $MgCl_2$).

Ribonuclease Treatment of the Immunoprecipitated Protein Complexes—The complexes bound to the agarose beads described above were incubated with 50 mM Tris-HCl pH 8.0, 150 mM NaCl, 5 mM $MgCl_2$ containing 10 μg/ml RNase A for 10 min at 37 °C, incubated for 30 min on ice, washed twice with lysis buffer and once with 50 mM Tris-HCl pH 8.0, 150 mM NaCl, and 5 mM $MgCl_2$, and eluted with buffer containing the FLAG peptide as described above.

Sucrose Density Gradient Ultracentrifugation—Sucrose density gradient ultracentrifugation was performed as described (41). Briefly, after removing the cytoplasm by the method described above, the pellet was sonicated in sonication buffer (25 mM Tris-HCl pH 8.0, 100 mM KCl, 1 mM NaF, 2 mM EDTA, 1 mM dithiothreitol, 0.05% IGEPAL CA-630, 1 mM PMSF, and 20 U SUPERase·In) three times for 20 s at 4 °C with a Bioruptor at the highest setting, and centrifuged for 15 min at 15,000 × *g*. The prepared Nu (1 mg) was overlaid on 9.5 ml of a 10–30% (w/w) sucrose gradient in 25 mM Tris-HCl pH 8.0, containing 100 mM KCl, 2 mM EDTA, and 1 mM dithiothreitol, and centrifuged at 36,000 rpm (average 162,000 × *g*) for 3 h at 4 °C in a Hitachi P40ST rotor, and separated into 20 fractions (500 μl each). The absorbance at 254 nm in each fraction was measured by Nano-Drop spectrophotometer (Thermo SCIENTIFIC, Wilmington, USA), and graphed by Excel. Proteins from each fraction were precipitated by 10% trichloroacetic acid before SDS-PAGE and immunoblot analysis. RNAs were prepared by addition to an equal volume of denaturing buffer (7 M urea, 350 mM NaCl, 10 mM EDTA, 10 mM Tris-HCl pH 8.0, 1% SDS, 2% 2-mercaptoethanol), to which was added 1/10 volume of 2 M sodium acetate (pH 4.0). The samples were vortexed, extracted by acidic phenol-chloroform, and precipitated with isopropanol. Ribosomal RNAs (18S, 28S, and 32S) were visualized with 0.02% methylene blue after transffered to Hybond N+ membrane (GE Healthcare) in 50 mM sodium acetate buffer (pH 5.5) for 10 min.

Immunofluorescence Staining—293EBNA cells were grown on collagen-coated culture slides and transfected with expression plasmids by the calcium phosphate method. To visualize whole cells, the transfected and intact cells were washed with PBS followed by fixation with 3.7% formaldehyde in PBS for 10 min at room temperature. After washing twice with PBST (0.05% (w/v) Tween 20), the cells were permeabilized with PBS containing 0.5% (w/v) Triton X-100 for 5 min at room temperature and washed once with PBST. To visualize nuclei, the transfected and intact cells were washed with PBS followed by permeabilization with PBS containing 0.5% (w/v) Triton

FIG. 1. **Association of p32 with several proteins involved in ribosome biogenesis.** *A*, Equivalent amounts of cytoplasmic (Cyto) or nuclear (Nu) extract prepared from mock- or p32-FLAG (p32)-transfected 293EBNA cells were analyzed by immunoblotting (IB) with anti-GAPDH as a marker of the cytoplasm, anti-Lamin B as a marker of the nucleus, and anti-FLAG for the detection of the expressed p32-FLAG. *B*, Nuclear extracts prepared from 293EBNA cells transfected with a plasmid containing a FLAG- (mock) or p32-FLAG-encoded DNA fragment (p32) were subjected to immunoprecipitation with anti-FLAG-fixed beads. The isolated proteins as well as an aliquot of the nuclear extract of mock- or p32-FLAG-transfected cells (input, 5 μg) were analyzed by 10% SDS-PAGE and visualized by silver staining. The asterisk indicates p32-FLAG used as bait. The molecular masses (kDa) are indicated at the left side of the figure. *C*, Association of p32-FLAG with the proteins identified by LC-MS/MS analysis and presence of ASF/SF2 was confirmed by immunoblot analysis with the indicated antibodies. *D*, The presence of known pre-rRNA processing factors that were not identified by LC-MS/MS analysis was examined by immunoblot analysis of the isolated p32-FLAG-associated proteins with the indicated antibodies.

TABLE I

The Nuclear p32-associated proteins that are involved or expected to be involved in ribosome biogenesis. The nuclear p32-associated proteins involved or expected to be involved in ribosome biogenesis are indicated. Proteins are classified into functional groups based on SwissProt classification. Proteins were identified by LC-MS/MS (LTQ-Orbitrap XL or Q-Tof2) and/or immunoblot analysis (IB), as described in Supplementary Tables I and II, and Figs. 1C and 1D. Proteins detected in mock are not listed in this table. Uniprot KB accession numbers, entry names, protein names as well as gene symbols are shown. For proteins having yeast orthologs, the gene names are indicated (obtained by Blink analysis of the NCBI database). Cellular localization is also indicated: No, nucleoli; Nm, nuclear membrane; Np, nucleoplasm; Nu, nucleus; Cy, cytoplasm; CBs, Cajal bodies

	Uniprot KB accession	Uniprot KB entry name	Protein name	Gene symbol	ID method			Cellular localization	Yeast homologs	[a]Function
					LTQ-Orbtrap XL	Q-Tof2	IB			
	pre-rRNAs modification and processing									
1	P22087	FBRL_HUMAN	rRNA 2∼-O-methyltransferase fibrillarin (FBL)[b]	FBL	○	○	○	No/CBs	NOP1	Pre-90S, pre-60S, boxC/D snoRNP, SSU processome, methyltransferase
2	O00567	NOP56_HUMAN	Nucleolar protein 56 (Nop56)	NOP56	○		○	No	NOP56	Pre-90S, boxC/D snoRNP, SSU processome
3	Q9Y2X3	NOP58_HUMAN	Nucleolar protein 58 (Nop58)	NOP58			○	No	NOP5	Pre-90S, boxC/D snoRNP, SSU processome
4	Q96G21	IMP4_HUMAN	U3 small nucleolar ribonucleoprotein protein IMP4	IMP4	○			No	IMP4	Pre-90S, U3 snoRNP, SSU processome
5	O00566	MPP10_HUMAN	U3 small nucleolar ribonucleoprotein protein MPP10	MPHOSPH10	○		○	No	MPP10	Pre-90S, U3 snoRNP, SSU processome
6	Q9BVI4	NOC4L_HUMAN	Nucleolar complex protein 4 homolog	NOC4L	○			No	NOC4	Pre-90S, SSU processome, Noc4-Nop14 complex function unknown in mammals
7	P78316	NOP14_HUMAN	Nucleolar protein 14	NOP14	○			No	NOP14	Pre-90S, SSU processome, Noc4-Nop14 complex function unknown in mammals
8	Q9NQZ2	SAS10_HUMAN	Something about silencing protein 10	UTP3	○			Nu	UTP3	Pre-90S, SSU processome, function unknown in mammals
9	Q9Y3A4	RRP7A_HUMAN	Ribosomal RNA-processing protein 7 homolog A	RRP7A	○			-	RRP7	Pre-90S, function unknown in mammals
10	P19338	NUCL_HUMAN	Nucleolin (NCL)	NCL			○	No	NSR1	Pre-90S, pre-60S
11	Q9NR30	DDX21_HUMAN	Nucleolar RNA helicase 2 (Guα)	DDX21	○	○	○	No	DBP1	Pre-60S, DEAD box RNA helicase
12	Q8N8A6	DDX51_HUMAN	ATP-dependent RNA helicase DDX51	DDX51	○			No	DBP6	Pre-60S, DEAD box RNA helicase
13	Q8IZL8	PELP1_HUMAN	Proline-, glutamic acid- and leucine-rich protein 1	PELP1	○			No/Nu/Cy	RIX1	Pre-60S, RIX1 complex, SENP3-sensitive target of SUMO
14	Q9NXF1	TEX10_HUMAN	Testis-expressed sequence 10 protein	TEX10	○			No/Nu/Nm	IPI1	Pre-60S, RIX1 complex
15	Q9BV38	WDR18_HUMAN	WD repeat-containing protein 18	WDR18	○			-	IPI3	pre-60S, RIX1 complex
16	Q9Y4W2	LAS1L_HUMAN	Protein LAS1 homolog	LAS1L	○	○		No	LAS1	Pre-60S, associated with human RIX1 complex, SENP3-sensitive target of SUMO
17	Q9NU22	MDN1_HUMAN	Midasin	MDN1	○			Nu	REA1	Pre-60S, associated with human RIX1 complex
18	Q9H4L4	SENP3_HUMAN	Sentrin-specific protease 3	SENP3	○			No/Np	ULP1	Pre-60S, associated with human RIX1 complex
19	Q5SY16	NOL9_HUMAN	Nucleolar protein 9	NOL9	○			No	GRC3	Pre-60S
20	P56182	RRP1_HUMAN	Ribosomal RNA processing protein 1 homolog A (Nop52)	RRP1	○	○	○	No	RRP1	Pre-60S, function unknown in mammals

10.1074/mcp.M110.006148–5

TABLE I—*continued*

	Uniprot KB accession	Uniprot KB entry name	Protein name	Gene symbol	ID method			Cellular localization	Yeast homologs	[a]Function
					LTQ-Orbtrap XL	Q-Tof2	IB			
21	Q8TDD1	DDX54_HUMAN	ATP-dependent RNA helicase DDX54	DDX54		○		No	DBP10	Pre-60S, DEAD box RNA helicase, function unknown in mammals
22	Q9NY93	DDX56_HUMAN	Probable ATP-dependent RNA helicase DDX56	DDX56	○			No	DBP9	Present in 65S preribosomal particles, DEAD box RNA helicase
23	Q9H6W3	NO66_HUMAN	Lysine-specific demethylase NO66	C14orf169	○	○		No/Np	-	Present in large preribosomal particles
24	Q5JTH9	RRP12_HUMAN	RRP12-like protein	RRP12	○	○		No/Nm	RRP12	Nuclear export of pre-40S and pre-60S, function unknown in mammals
25	Q9BQ39	DDX50_HUMAN	ATP-dependent RNA helicase DDX50 (Guβ)	DDX50	○	○	○	No	DBP1	DEAD box RNA helicase
26	Q01780	EXOSX_HUMAN	Exosome component 10 (PM/Scl-100)	EXOSC10			○	No/Cy	RRP6	Exosome
27	Q9NQT5	EXOS3_HUMAN	Exosome complex exonuclease RRP40	EXOSC3			○	No/Cy	RRP40	Exosome
28	Q9UI43	RRMJ2_HUMAN	Putative ribosomal RNA methyltransferase 2 (FTSJ2)	FTSJ2			○	No	MRM2	Methyltransferase
	Nucleolar Protein									
29	Q9BQG0	MBB1A_HUMAN	Myb-binding protein 1A	MYBBP1A	○			No/Cy	POL5	
30	Q5C9Z4	NOM1_HUMAN	Nucleolar MIF4G domain-containing protein 1	NOM1	○	○		No	SGD1	
31	Q14684	RRP1B_HUMAN	Ribosomal RNA processing protein 1 homolog B[b]	RRP1B	○			No	RRP1	

[a] Known roles in ribosome biogenesis and/or associated pre-ribosome particles for yeast homologs or for human proteins are indicated.
[b] The proteins known to be associated with p32.

TABLE II

The Nuclear p32-associated proteins that are not involved in ribosome biogenesis. The nuclear p32-associated proteins are indicated. Proteins are classified into functional groups based on SwissProt classification. Proteins were identified by LC-MS/MS (LTQ-Orbitrap XL or Q-Tof2) and/or immunoblot analysis (IB), as described in Supplementary Tables I and II, and Figs. 1C and 1D. Proteins detected in mock are not listed in this table. Uniprot KB accession numbers, entry names, protein names as well as gene symbols are shown

	Uniprot KB accession	Uniprot KB Entry name	Protein name	Gene symbol	ID method		
					LTQ-Orbitrap XL	Q-Tof2	IB
	Chromatin remodeling						
1	Q969G3	SMCE1_HUMAN	SWI/SNF-related matrix-associated actin-dependent regulator of chromatin subfamily E member 1	SMARCE1	○		
2	Q12824	SNF5_HUMAN	SWI/SNF-related matrix-associated actin-dependent regulator of chromatin subfamily B member 1	SMARCB1	○		
3	O60264	SMCA5_HUMAN	SWI/SNF-related matrix-associated actin-dependent regulator of chromatin subfamily A member 5	SMARCA5	○		
4	Q8TAQ2	SMRC2_HUMAN	SWI/SNF complex subunit SMARCC2	SMARCC2	○	○	
5	Q92922	SMRC1_HUMAN	SWI/SNF complex subunit SMARCC1	SMARCC1	○		
6	Q86U86	PB1_HUMAN	Protein polybromo-1	PBRM1	○		
7	Q8WUB8	PHF10_HUMAN	PHD finger protein 10	PHF10	○		
8	P51610	HCFC1_HUMAN	Host cell factor 1	HCFC1	○		
9	Q6ZRS2	SRCAP_HUMAN	Helicase SRCAP	SRCAP	○		
10	Q9P2D1	CHD7_HUMAN	Chromodomain-helicase-DNA-binding protein 7	CHD7	○		
11	Q14839	CHD4_HUMAN	Chromodomain-helicase-DNA-binding protein 4	CHD4	○		
12	Q9NPI1	BRD7_HUMAN	Bromodomain-containing protein 7	BRD7	○		
13	Q68CP9	ARID2_HUMAN	AT-rich interactive domain-containing protein 2	ARID2	○		
	RNA polymerase III transcription						
14	Q12789	TF3C1_HUMAN	General transcription factor 3C polypeptide 1 (TFIIIC220)	GTF3C1	○	○	○
15	Q8WUA4	TF3C2_HUMAN	General transcription factor 3C polypeptide 2	GTF3C2	○	○	
16	Q9Y5Q9	TF3C3_HUMAN	General transcription factor 3C polypeptide 3 (TFIIIC102)	GTF3C3	○	○	○
17	Q9UKN8	TF3C4_HUMAN	General transcription factor 3C polypeptide 4	GTF3C4	○	○	
18	Q9Y5Q8	TF3C5_HUMAN	General transcription factor 3C polypeptide 5	GTF3C5	○	○	
19	O15318	RPC7_HUMAN	DNA-directed RNA polymerase III subunit RPC7	POLR3G			○
	Transcription						
20	Q9H869	YYAP1_HUMAN	YY1-associated protein 1	YY1AP1	○		
21	Q8WXI9	P66B_HUMAN	Transcriptional repressor p66-beta	GATAD2B	○		
22	Q13263	TIF1B_HUMAN	Transcription intermediary factor 1-beta	TRIM28	○		
23	P05412	JUN_HUMAN	Transcription factor AP-1	JUN	○		
24	P51532	SMCA4_HUMAN	Transcription activator BRG1	SMARCA4	○		
25	Q14498	RBM39_HUMAN	RNA-binding protein 39	RBM39	○		
26	Q8N7H5	PAF1_HUMAN	RNA polymerase II-associated factor 1 homolog	PAF1	○		
27	P30876	RPB2_HUMAN	DNA-directed RNA polymerase II subunit RPB2	POLR2B	○		
28	P15336	ATF2_HUMAN	Cyclic AMP-dependent transcription factor ATF-2	ATF2	○		
29	Q7RTS1	BHA15_HUMAN	Class A basic helix-loop-helix protein 15	BHLHA15	○		
	DNA binding/replication/repair						
30	Q14683	SMC1A_HUMAN	Structural maintenance of chromosomes protein 1A	SMC1A	○		
31	P12004	PCNA_HUMAN	Proliferating cell nuclear antigen	PCNA	○		
32	Q9Y2S7	PDIP2_HUMAN	Polymerase delta-interacting protein 2	POLDIP2	○		
33	Q9UBB5	MBD2_HUMAN	Methyl-CpG-binding domain protein 2	MBD2	○		
34	O00255	MEN1_HUMAN	Menin	MEN1	○		
35	P78527	PRKDC_HUMAN	DNA-dependent protein kinase catalytic subunit	PRKDC	○		
36	P26358	DNMT1_HUMAN	DNA (cytosine-5)-methyltransferase 1	DNMT1	○		
37	Q7Z7K6	CENPV_HUMAN	Centromere protein V	CENPV	○		
38	Q53HL2	BOREA_HUMAN	Borealin	CDCA8	○		
	mRNA splicing/stabilization						
39	Q07955	SRSF1_HUMAN	Serine/arginine-rich splicing factor 1 (ASF/SF2)[a]	SRSF1			○
40	O95104	SFR15_HUMAN	Splicing factor, arginine/serine-rich 15	SFRS15	○		
41	Q99590	SFRIP_HUMAN	SFRS2-interacting protein	SRSF2IP	○		
42	Q86U06	RBM23_HUMAN	Probable RNA-binding protein 23	RBM23	○		
43	P09651	ROA1_HUMAN	Heterogeneous nuclear ribonucleoprotein A1 (hnRNP A1)[a]	HNRNPA1		○	○
44	P48634	BAT2_HUMAN	Large proline-rich protein BAT2[a]	BAT2	○	○	
45	Q14004	CDK13_HUMAN	Cell division protein kinase 13[a]	CDK13	○		
	RNA binding protein						
46	Q9NQ29	LUC7L_HUMAN	Putative RNA-binding protein Luc7-like 1	LUC7L	○		
47	Q9UHX1	PUF60_HUMAN	Poly(U)-binding-splicing factor PUF60	PUF60	○		
48	P51116	FXR2_HUMAN	Fragile X mental retardation syndrome-related protein 2	FXR2	○		
49	Q06787	FMR1_HUMAN	Fragile X mental retardation 1 protein	FMR1	○		

TABLE II—*continued*

	Uniprot KB accession	Uniprot KB Entry name	Protein name	Gene symbol	ID method		
					LTQ-Orbitrap XL	Q-Tof2	IB
	Telomere						
50	Q9NYB0	TE2IP_HUMAN	Telomeric repeat-binding factor 2-interacting protein 1	TERF2IP	○		
51	Q15554	TERF2_HUMAN	Telomeric repeat-binding factor 2	TERF2	○		
	Nuclear envelop/pore/lamina						
52	Q5SNT2	TM201_HUMAN	Transmembrane protein 201	TMEM201	○		
53	O94901	SUN1_HUMAN	SUN domain-containing protein 1	SUN1	○		
54	Q8N1F7	NUP93_HUMAN	Nuclear pore complex protein Nup93	NUP93	○		
55	Q92621	NU205_HUMAN	Nuclear pore complex protein Nup205	NUP205	○		
56	Q12769	NU160_HUMAN	Nuclear pore complex protein Nup160	NUP160	○		
57	Q8WUM0	NU133_HUMAN	Nuclear pore complex protein Nup133	NUP133	○		
58	P57740	NU107_HUMAN	Nuclear pore complex protein Nup107	NUP107	○		
59	Q96HA1	P121A_HUMAN	Nuclear envelope pore membrane protein POM 121	POM121	○		
60	Q14739	LBR_HUMAN	Lamin-B receptor[a]	LBR	○		
	Protein glycosylation						
61	P39656	OST48_HUMAN	Dolichyl-diphosphooligosaccharide-protein glycosyltransferase 48 kDa subunit	DDOST	○		
62	P04843	RPN1_HUMAN	Dolichyl-diphosphooligosaccharide-protein glycosyltransferase subunit 1	RPN1	○		
	Importin						
63	P52292	IMA2_HUMAN	Importin subunit alpha-2	KPNA2	○		
64	P52294	IMA1_HUMAN	Importin subunit alpha-1	KPNA1	○		
	Mitochondorial protein						
	OXPHOS complex						
65	P21912	DHSB_HUMAN	Succinate dehydrogenase [ubiquinone] iron-sulfur subunit, mitochondrial	SDHB	○		
66	P31040	DHSA_HUMAN	Succinate dehydrogenase [ubiquinone] flavoprotein subunit, mitochondrial	SDHA	○		
67	O75306	NDUS2_HUMAN	NADH dehydrogenase [ubiquinone] iron-sulfur protein 2, mitochondrial	NDUFS2	○		
68	P36542	ATPG_HUMAN	ATP synthase subunit gamma, mitochondrial	ATP5C1	○		
	Mitochondrial membrane protein						
69	Q9Y277	VDAC3_HUMAN	Voltage-dependent anion-selective channel protein 3	VDAC3	○		
70	P45880	VDAC2_HUMAN	Voltage-dependent anion-selective channel protein 2	VDAC2	○		
71	P21796	VDAC1_HUMAN	Voltage-dependent anion-selective channel protein 1	VDAC1	○	○	
72	Q9H9B4	SFXN1_HUMAN	Sideroflexin-1	SFXN1	○		
73	O96008	TOM40_HUMAN	Mitochondrial import receptor subunit TOM40 homolog	TOMM40	○		
74	O75746	CMC1_HUMAN	Calcium-binding mitochondrial carrier protein Aralar1	SLC25A12	○		
75	Q9Y4W6	AFG32_HUMAN	AFG3-like protein 2	AFG3L2	○		
	Lipid metabolism						
76	P40939	ECHA_HUMAN	Trifunctional enzyme subunit alpha, mitochondrial	HADHA	○		
77	P55084	ECHB_HUMAN	Trifunctional enzyme subunit beta, mitochondrial	HADHB	○		
	Others						
78	P42704	LPPRC_HUMAN	Leucine-rich PPR motif-containing protein, mitochondrial	LRPPRC	○		
79	Q96EY1	DNJA3_HUMAN	DnaJ homolog subfamily A member 3, mitochondrial	DNAJA3	○		
80	O00411	RPOM_HUMAN	DNA-directed RNA polymerase, mitochondrial	POLRMT	○		
81	Q96TA2	YMEL1_HUMAN	ATP-dependent metalloprotease YME1L1	YME1L1	○		
82	O76031	CLPX_HUMAN	ATP-dependent Clp protease ATP-binding subunit clpX-like, mitochondrial	CLPX	○		
83	O95831	AIFM1_HUMAN	Apoptosis-inducing factor 1, mitochondrial	AIFM1	○		
	ER protein						
84	P43307	SSRA_HUMAN	Translocon-associated protein subunit alpha	SSR1	○		
85	Q9UGP8	SEC63_HUMAN	Translocation protein SEC63 homolog	SEC63	○		
86	P55072	TERA_HUMAN	Transitional endoplasmic reticulum ATPase	VCP	○		
87	Q9NZ01	TECR_HUMAN	Trans-2,3-enoyl-CoA reductase	TECR	○		
88	P16615	AT2A2_HUMAN	Sarcoplasmic/endoplasmic reticulum calcium ATPase 2	ATP2A2	○		
89	Q13724	MOGS_HUMAN	Mannosyl-oligosaccharide glucosidase	MOGS	○		
	Others						
90	Q15836	VAMP3_HUMAN	Vesicle-associated membrane protein 3	VAMP3	○		
91	Q93009	UBP7_HUMAN	Ubiquitin carboxyl-terminal hydrolase 7	USP7	○		
92	P07437	TBB5_HUMAN	Tubulin beta chain	TUBB	○		
93	Q14232	EI2BA_HUMAN	Translation initiation factor eIF-2B subunit alpha	EIF2B1	○		
94	Q07157	ZO1_HUMAN	Tight junction protein ZO-1	TJP1	○		
95	P48594	SPB4_HUMAN	Serpin B4	SERPIN B4	○		

TABLE II—*continued*

	Uniprot KB accession	Uniprot KB Entry name	Protein name	Gene symbol	ID method		
					LTQ-Orbitrap XL	Q-Tof2	IB
96	P29508	SPB3_HUMAN	Serpin B3	SERPIN B3	○		
97	P48651	PTSS1_HUMAN	Phosphatidylserine synthase 1	PTDSS1	○		
98	Q15758	AAAT_HUMAN	Neutral amino acid transporter B(0)	SLC1A5	○		
99	Q8NFW8	NEUA_HUMAN	N-acylneuraminate cytidylyltransferase	CMAS	○		
100	Q8WVX9	FACR1_HUMAN	Fatty acyl-CoA reductase 1	FAR1	○		
101	P35613	BASI_HUMAN	Basigin	BSG	○		
102	P06733	ENOA_HUMAN	Alpha-enolase	ENO1	○		
	Unknown						
103	Q96JP5	ZFP91_HUMAN	Zinc finger protein 91 homolog	ZFP91	○	○	
104	Q9H5H4	ZN768_HUMAN	Zinc finger protein 768	ZNF768	○		
105	Q14966	ZN638_HUMAN	Zinc finger protein 638	ZNF638	○		
106	Q8NAF0	ZN579_HUMAN	Zinc finger protein 579	ZNF579	○		
107	Q5VZL5	ZMYM4_HUMAN	Zinc finger MYM-type protein 4	ZMYM4	○		
108	Q8N9Z2	YG034_HUMAN	Uncharacterized protein FLJ36031	FLJ36031	○		
109	Q9Y4P3	TBL2_HUMAN	Transducin beta-like protein 2	TBL2	○		
110	Q9UJZ1	STML2_HUMAN	Stomatin-like protein 2	STOML2	○		
111	Q9P2N5	RBM27_HUMAN	RNA-binding protein 27	RBM27	○		
112	Q5T8P6	RBM26_HUMAN	RNA-binding protein 26	RBM26	○		
113	Q9NWS8	RMND1_HUMAN	Required for meiotic nuclear division protein 1 homolog	RMND1	○		
114	Q6P158	DHX57_HUMAN	Putative ATP-dependent RNA helicase DHX57	DHX57	○		
115	Q69YN4	VIR_HUMAN	Protein virilizer homolog	KIAA1429	○		
116	Q9BX40	LS14B_HUMAN	Protein LSM14 homolog B	LSM14B	○		
117	Q9Y520	BA2L2_HUMAN	Protein BAT2-like 2	BAT2L2	○		
118	Q9ULL5	PRR12_HUMAN	Proline-rich protein 12	PRR12	○		
119	Q96DN6	MBD6_HUMAN	Methyl-CpG-binding domain protein 6	MBD6	○		
120	Q9UNF1	MAGD2_HUMAN	Melanoma-associated antigen D2	MAGED2	○		
121	Q9NXS2	QPCTL_HUMAN	Glutaminyl-peptide cyclotransferase-like protein	QPCTL	○		
122	Q96SL8	FIZ1_HUMAN	Flt3-interacting zinc finger protein 1	FIZ1	○		
123	Q68CQ4	DEF_HUMAN	Digestive organ expansion factor homolog	C1orf107	○		
124	Q9H0W5	CCDC8_HUMAN	Coiled-coil domain-containing protein 8	CCDC8	○		

[a] The proteins known to be associated with p32.

X-100 for 10 min at room temperature. After washing twice with PBST, the cells were fixed with 3.7% formaldehyde in PBS for 10 min at room temperature and washed twice with PBST. The cells were then blocked with 3% (w/v) nonfat dried milk in PBS for 1 h, and incubated with the appropriate primary antibody for 1 h at room temperature. The cells were washed three times in PBST for 10 min and then incubated with fluorochrome-conjugated secondary antibody for 1 h at room temperature. The cells were washed three times in PBST for 10 min and then mounted with Vectashield. The resulting cells were examined with an Axiovert 200 M microscope (Carl Zeiss, Germany).

Protein Identification by Liquid Chromatography-Tandem MS (LC-MS/MS) Analysis—Pulled-down proteins were separated on a gel by SDS-PAGE; the gel was cut into five pieces, each of which was subjected to in-gel digestion with trypsin (36), and the resulting peptides were analyzed using a nanoscale LC-MS/MS system with quadrupole-time-of-flight (Q-Tof)2 hybrid mass spectrometer (Q-Tof 2, Micromass, Wythenshawe, UK) as described (39, 42). The peptide mixture was applied to a Mightysil-RP-18 (3 μm particle, Kanto Chemical, Osaka, Japan) fritless column (45 mm $\times$ 0.150 mm i.d.) and separated using a 0–40% gradient of acetonitrile containing 0.1% formic acid over 80 min at a flow rate of 50 nl/min. Eluted peptides were sprayed directly into Q-Tof2. The peptides were detected in the MS mode to select a set of precursor ions for a data-dependent, collision-induced dissociation (CID) mass spectrometric (MS/MS) analysis, and every 4 s the four ions having the greatest signal intensity were subjected to the MS/MS analysis. The MS/MS signals were acquired by MassLynx version 3.5 (Micromass, UK) and converted to text files by ProteinLynx software (Micromass). The database search was performed by MASCOT version 2.2.1 (Matrix Science Ltd., London, UK) against the Uniprot human proteins databases Sprot 57.5, 471472 sequences, with the following parameters: fixed modification; carbamidemethyl (Cys), variable modifications: oxidation (Met), N-acetylation, pyroglutamine; maximum missed cleavages: 1; peptide mass tolerance: 200 ppm; MS/MS tolerance: 0.3 Da. The criteria were based on the vendor's definitions (Matrix Science, Ltd.). Furthermore, we set more strict criteria for protein assignment: (i) any peptide candidate with an MS/MS signal number of <2 was eliminated from the 'hit' candidates, regardless of the match score (total score minus threshold); and (ii) more than two peptides containing at least one peptide with ion score over 33 ($p < 0.05$) plus peptide(s) with ion score over 10 were considered as 'hit'.

We also performed LC-MS/MS analysis with LTQ-Orbitrap hybrid mass spectrometer (model XL, Thermo Fisher Scientific, CA, USA). The mass spectrometer was operated in a data-dependent mode to automatically switch between Orbitrap-MS and linear ion trap-MS/MS acquisition. Survey full scan MS spectra (from *m/z* 450 to 1500) acquired in the Orbitrap with resolution $r = 15{,}000$ (after accumulation to a target value of 500,000 ions in the linear ion trap). The most intense ions (up to ten, depending on signal intensity) were sequentially isolated for fragmentation for every 0.2 s in the linear ion trap using CID at a target value of 30,000 ions. An MS scan and an MS/MS scan was one with centroid. The resulting fragment ions were recorded in the linear ion trap with a normal mode. Target ions selected for MS/MS were dynamically excluded for 30 s while the difference of 10 ppm. General mass spectrometric conditions were as follows: electrospray voltage, 1.6 kV; no lock mass option; with sheath and auxiliary gas flow; normalized collision energy, 35% for MS/MS. Ion selection threshold was 10 000 counts for MS/MS. An activation q-value of 0.25 and activation time of 30 ms was applied for MS/MS acquisitions.

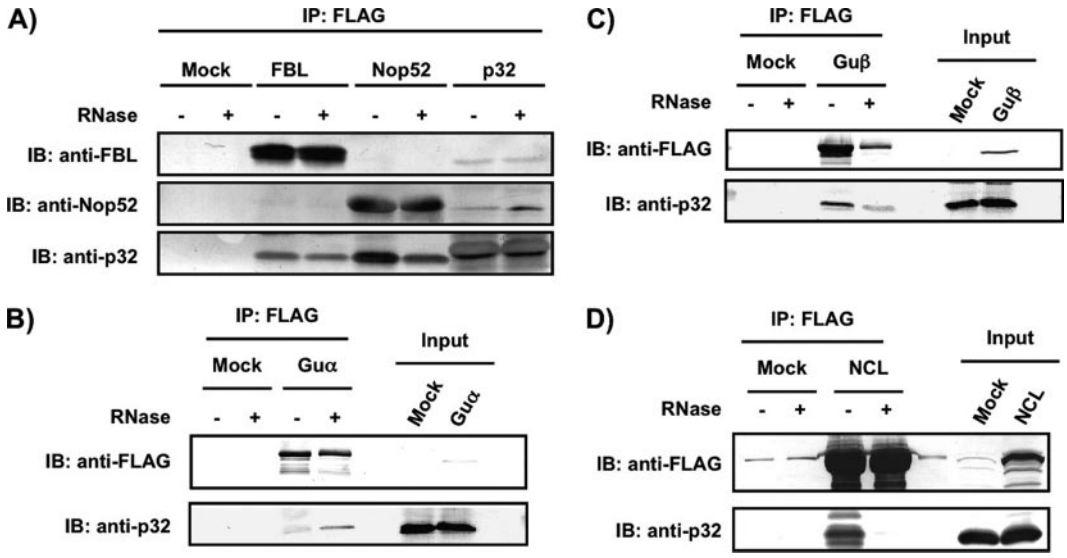

FIG. 2. **Reciprocal association of FBL, Nop52, Guα, Guβ, or NCL with p32.** Proteins were immunoprecipitated with anti-FLAG from the whole-cell extract of 293EBNA cells expressing FLAG-tagged FBL (*A*), Nop52 (A), Guα (*B*), Guβ (*C*), or nucleolin (NCL) (*D*), and detected by immunoblotting (IB) with anti-FBL, anti-Nop52, anti-FLAG or anti-p32 before (–) and after (+) treatment with RNase A. Input: 30 μg of an aliquot of whole-cell extract.

The raw data acquired by Xcalibur version 2.0.7 (Thermo Fisher Scientific, USA) was converted to mgf file by Proteome Discoverer version 1.1 (Thermo Fisher Scientific). The database search was performed by MASCOT version 2.2.07 against the Uniprot human database version SwissProt_2010_05, 516603 sequences, with the following parameters: fixed modification; carbamidemethyl (Cys), variable modifications: oxidation (Met), N-acetylation, pyroglutamine; maximum missed cleavages: 1; peptide mass tolerance 10 ppm; MS/MS tolerance: 0.8 Da. We selected the candidate peptides with probability-based Mowse scores (total score) that exceed its threshold indicating a significant homology ($p < 0.05$; score over 20), and referred to them as "hits." The criteria were based on the vendor's definitions. Furthermore, we set more strict criteria for protein assaignment: (1) any peptide candidate with an MS/MS signal number of <2 was eliminated from the 'hits' candidates, regardless of the match score (total score minus threshold); (2) proteins with match scores under 100 were also eliminated from the hits candidates. Peptides that are shared within a group of proteins were excluded from peptide assignment lists in supplemental Tables S1 and S2.

As a control, FLAG tag bound to anti-FLAG M2 agarose beads was also pulled down with the Nu. The proteins released from the M2 beads by eluting with FLAG peptide were separated by SDS-PAGE and subjected to in-gel trypsin digestion-LC-MS/MS analysis as described above, and were subtracted from the proteins identified in the total FLAG-tagged protein-associated complexes; thus, those proteins identified in the FLAG-tag eluate were not included in the FLAG-tagged protein-associated proteins unless the quantitative increase was confirmed.

Proliferation Assay—The siRNA615-transfected HeLa cells were counted 24 h after second transfection. Cells (5.0×10^3) were placed into new 24-well plates and incubated for various times. At proper time point, the cells were incubated with 0.1 μCi/ml [methyl-^{3}H]Thymidine (PerkinElmer, NET 027E) for 1 h. After a brief rinse with ice-cold PBS, 10% trichloroacetic acid were added and incubated on ice for 30 min for DNA precipitation. The precipitated DNA were washed with 10% trichloroacetic acid, and incubated with 0.1 N NaOH, 1% SDS solution at 37 °C for 30 min for solubilization. The [methyl-^{3}H]Thymidine incorporation into DNA was measured by scintillation counting with Insta-Gel Plus (PerkinElmer, Waltham, MA).

Metabolic Labeling and Analysis of RNA Transcripts—For [^{3}H]uridine labeling, subconfluent siRNA-transfected HeLa cells in 35-mm dishes were incubated with 3 μCi/ml [5,6-^{3}H]uridine (PerkinElmer, NET367) for 2 h. After a brief rinse with ice-cold PBS, total RNA was isolated using the RNAgent total RNA isolation system (Promega, Madison, WI) according to the manufacturer's instructions, and the incorporation of [^{3}H]uridine was measured with Insta-Gel Plus by scintillation counting. RNA concentration was determined by NanoDrop. An aliquot of RNA with an equal count (20,000 cpm) of the [^{3}H]uridine incorporation from each sample was loaded on each lane of a 0.7% agarose/formaldehyde gel and electrophoresed in 3-(*N*-morpholino)propanesulfonic acid (MOPS) running buffer at 3.5 V/cm for 5 h for analysis of large rRNAs, and a 10% polyacrylamide/7.5 M urea gel in TBE running buffer at 15 V/cm for 3.5 h for small RNAs. Separated RNAs were transferred to a Hybond N+ membrane, which was subsequently dried and sprayed by EN^{3}HANCE (PerkinElmer) and exposed to a Kodak BioMax MS film (Kodak) for 3 days in a deep freezer. For metabolic labeling of RNA with [^{3}H]uridine, sub-confluent siRNA-transfected HeLa cells in a 35-mm dish were incubated for 30 min in medium containing [^{3}H]uridine (5 μCi/ml). The cells were then chased in medium containing 0.5 mM nonradioactive uridine, after which RNA was isolated using RNAgent, and the RNAs were analyzed as described above. For [^{3}H]uridine labeling of RNAs in the p32-associated complex, Flp-In T-REx 293 cells or those stably expressed p32-FLAG were incubated with 3 μCi/ml [5,6-^{3}H]uridine for 2 h in 90-mm dishes, harvested from six dishes, and lysed as described above in 1 ml $MgCl_2$-free lysis buffer containing 1 mM PMSF and 20 U SUPERase·In. The soluble fraction was obtained by centrifugation at 12,000 $\times$ *g* for 10 min at 4 °C, and was incubated with 10 μl anti-FLAG M2 agarose beads for 2 h at 4 °C. After washing the agarose beads with $MgCl_2$-free lysis buffer, the RNAs in the complexes bound to the agarose beads or soluble cell lysates were extracted using the RNAgent, and were analyzed as described above.

Northern Blot Hybridization—RNAs were extracted from the p32-associated complex using the RNAgent, and were electrophoresed

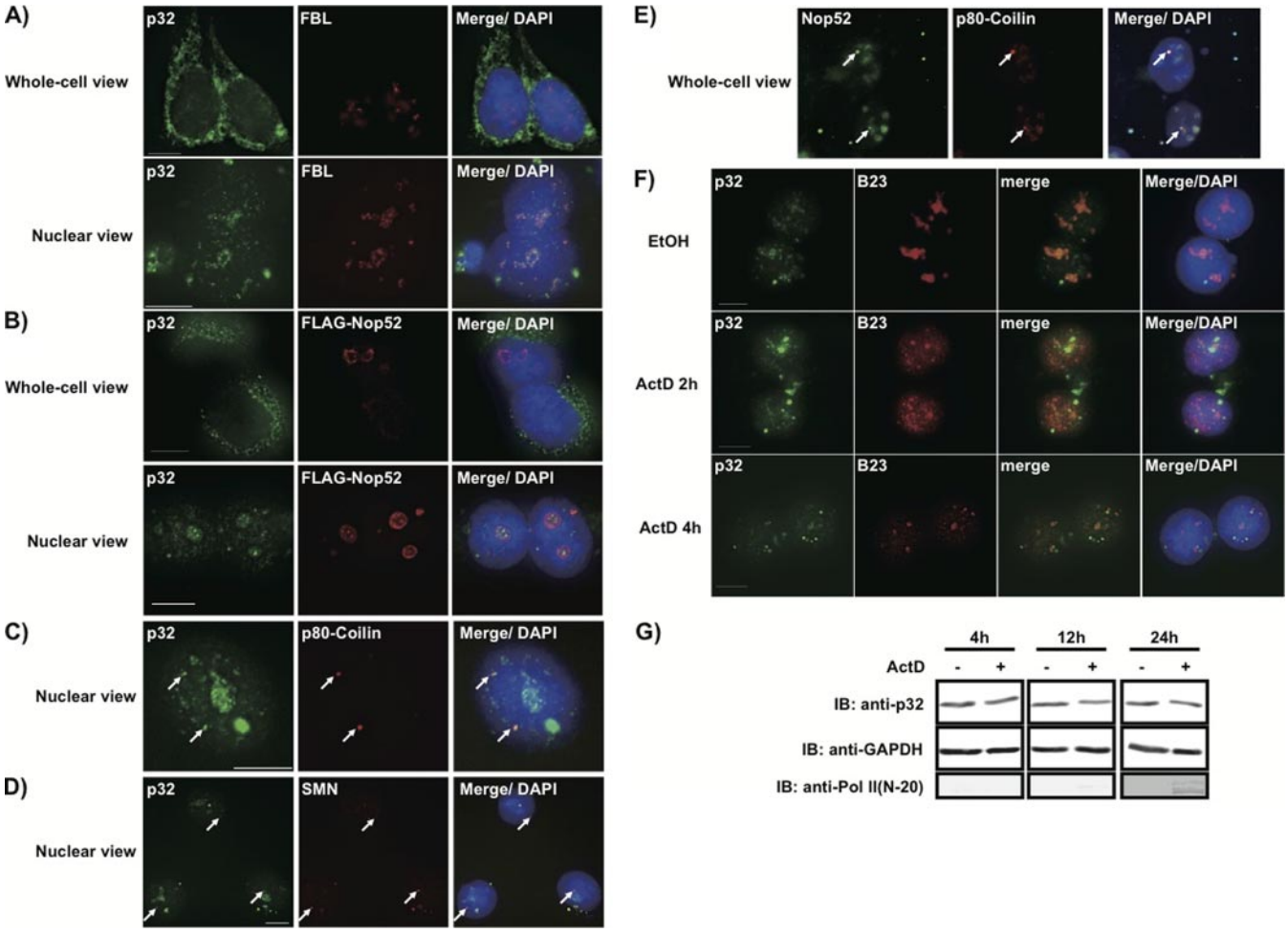

FIG. 3. **Co-localization of endogenous p32 with FBL and Nop52 in the nucleolus and Cajal bodies, and exclusion of p32 from the nucleolus by actinomycin D treatment.** 293EBNA cells were fixed before (whole-cell view) or after (nuclear view) permeabilization and immunostained using an antibody against p32, FBL, FLAG, Nop52, p80-coilin, or SMN. p32, corresponding immunolocalization of endogenous p32. FBL, corresponding images stained for FBL indicating dense fibrillar component (DFC) of the nucleoli. FLAG-Nop52 and Nop52, corresponding images stained for FLAG-Nop52 and endogenous Nop52, respectively, indicating granular component (GC) of the nucleoli. p80-coilin, corresponding images stained for p80-coilin indicating Cajal bodies. SMN, corresponding images stained for SMN indicating Cajal bodies. Merge/DAPI for (A)~(D), merge of p32 and DAPI, and FBL (*A*), or FLAG-Nop52 (*B*), or p80-coilin (*C*), or SMN (*D*). Merge/DAPI for (*E*), merge of Nop52 and DAPI, and p80-coilin. *F*, 293EBNA cells were treated with 2 μg/ml actinomycin D (ActD) for 2 h or 4 h, and stained for analysis by indirect immunofluorescence (p32 in green; B23 in red). Ethanol, treated with ethanol for 4 h. Merge/DAPI, merge of p32, B23, and DAPI. Bars indicate 10 μm. *G*, Total proteins from cells treated for longer periods with ActD analyzed by immunoblotting with the antibodies indicated at the left. Pol II (N-20), RNA polymerase II (antibody against hypo- and hyper-phosphorylated forms of Pol II).

with agarose gel and transferred to a Hybond N+ membrane as described above. After stained with methylene blue, the membrane was hybridized to biotin-labeled probes at 50 °C overnight in pre-hybridization solution (5× SSC, 20 mM Na_2HPO_4 pH 7.2, 7% SDS, 2 X Denhardt's Solution, 1 mg/ml salmon sperm DNA). The membrane was washed with NonStringent wash solution (3× SSC, 25 mM NaH_2PO_4 (pH 7.5), 5% SDS) once for 10 min at 50 °C, twice for 30 min at 50 °C, and once with Stringent wash solution (1× SSC, 1% SDS) for 15 min at 50 °C. The hybridized RNA was detected by using Chemiluminescent Nucleic Acid Detection Module Kit (Thermo). The following oligonucleotides were used as probes to detect human pre-rRNAs in Northern blot hybridization (see Fig. 4*D*): 5′ ETS probe (5′- ACAGCGACGGAGGCAATACC-3′) to nt 1468 to 1487 of the 5′ ETS; ITS1 probe (5′-AACGCGCTAGGTACCTGGACGG-3′) to nt 586 to 607 of the ITS1; 5.8S probe (5′- AGACAGGCGTAGCCCCGGGAG-GAA -3′) to nt 123 to 146 of the 5.8S; ITS2 probe (5′- ACGCCGC-CGGGTCTGCGCTTA-3′) to nt 93 to 113 of the ITS2. Probes were 3′-end labeled using Biotin 3′ End DNA Labeling Kit (Thermo).

Purification of GST-Fusion Proteins and In Vitro Binding Assay—GST-fusion proteins were prepared based on the method described by Fujiyama-Nakamura and Yoshikawa *et al.* (39). Briefly, *Escherichia coli* BL21 (DE3) strain carrying a pGEX 4T plasmid encoding GST, GST-fused p32 (GST-p32), GST-thrombin cleavage site-FBL, or GST-thrombin cleavage site-FLAG-Nop52 was grown in 250 ml of Luria-Bertani medium, was treated with isopropyl β-D-thiogalactoside (final concentration 0.1 mM) for 4 h at 25 °C, and collected by centrifugation. The cells were suspended in 10 ml of PBS containing 2 mM EDTA, 0.1% 2-mercaptoethanol, and 0.5 mM PMSF, divided into 3 tubes, and sonicated for 20 s × 18 times at 4 °C with a Bioruptor at the high setting with a microtip. Cell lysate in each tube was centrifuged for 20 min at 20,000 × *g*. The supernatant (10 ml) was mixed with 200 μl of a 50% (v/v) slurry of glutathione-Sepharose-4B beads

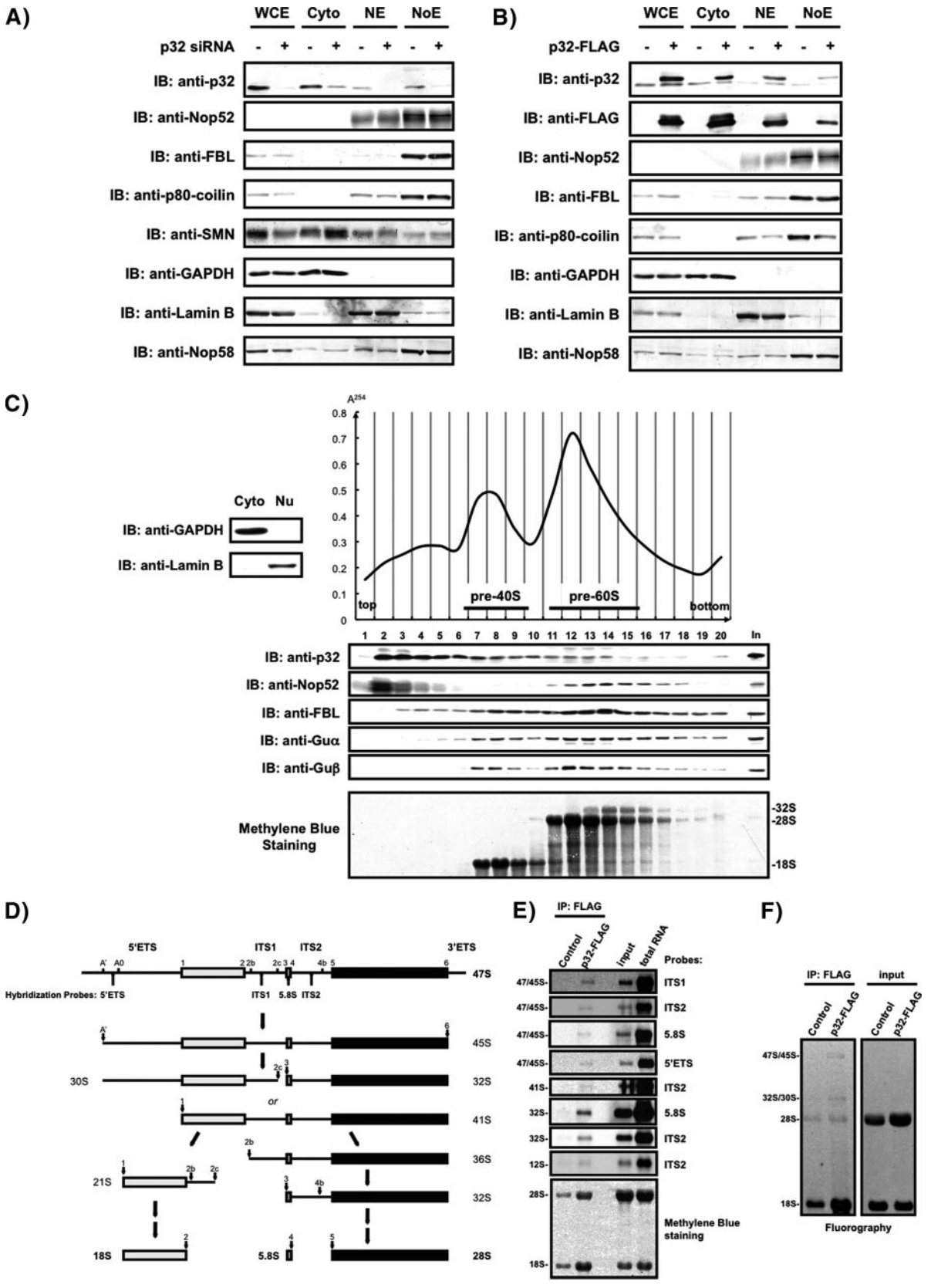
A)
WCE
Cyto
NE
NoE
p32 siRNA
IB: anti-p32
IB: anti-Nop52
IB: anti-FBL
IB: anti-p80-coilin
IB: anti-SMN
IB: anti-GAPDH
IB: anti-Lamin B
IB: anti-Nop58
B)
p32-FLAG
IB: anti-FLAG
C)
Cyto Nu
top
pre-40S
pre-60S
bottom
In
IB: anti-Guα
IB: anti-Guβ
Methylene Blue Staining
-32S
-28S
-18S
D)
5'ETS
ITS1
ITS2
3'ETS
47S
Hybridization Probes: 5'ETS
45S
30S
32S
or
41S
36S
21S
18S
5.8S
28S
E)
IP: FLAG
Control
p32-FLAG
input
total RNA
Probes:
ITS1
ITS2
5.8S
5'ETS
Methylene Blue staining
F)
IP: FLAG
input
Fluorography

(GE Healthcare). The GST-protein-bound beads were washed with PBS containing 2 mM EDTA, 0.1% 2-mercaptoethanol, 0.5 mM PMSF, and 2% Tween 20 until absorbance at 280 nm in flow through became zero. FLAG-Nop52 or FBL was eluted from the beads by centrifugation after the cleavage with thrombin (final concentration 1%) for 2 h at 25 °C. GST or GST-p32 were mixed with the isolated FLAG-Nop52, or FBL, and incubated with glutathione-Sepharose-4B beads for 1 h at 4 °C. The beads were centrifuged, washed five times with 1 ml lysis buffer and once more with 50 mM Tris-HCl pH 8.0, containing 150 mM NaCl and 5 mM $MgCl_2$. Proteins bound to glutathione-Sepharose-4B beads were separated by SDS-PAGE and detected by coomassie brilliant blue (CBB, quick-CBB WAKO) staining or by immunoblot analysis with anti-FLAG antibody, or anti-FBL antibody.

RESULTS

p32 Associates with Many Pre-rRNA Processing Factors Including Nop52—We first confirmed that p32-FLAG and endogenous p32 had the same subcellular localization (supplemental Fig. S1). We pulled down p32-FLAG-associated proteins from the Nu of 293EBNA cells (Figs. 1*A* and 1*B*), carried out nano-LC-MS/MS analyses of the p32-FLAG-associated proteins, and assigned the obtained MS/MS spectra to proteins using the Mascot search software (39) (supplemental Tables S1 and S2). We identified 149 proteins by these MS/MS analyses (Tables I and II and supplemental Tables S1 and S2). To confirm the mass-based identification, we also performed immunoblot analyses of the p32-FLAG-associated proteins using antibodies to the identified proteins against Nop52, Nop56, FBL, Mpp10, RNA helicases Guα and Guβ, TFIIIC220, TFIIIC102, and hnRNP A1, and detected all the proteins examined by the mass-based analysis (Fig. 1*C*). Mass-based analysis identified the six known nuclear p32-binding proteins (lamin B receptor, FBL, hnRNPA1, BAT2, RRP1B, and CDK13) (2, 3, 16, 26, 43, 44), and identified 143 proteins as new candidates that associate with p32. Although the mass-based analysis did not identify ASF/SF2, which is known as the nuclear p32-binding protein, we detected it among the p32-FLAG-associated proteins by immunoblotting using anti-ASF/SF2 (Fig. 1*C*). Among the proteins identified by mass-based analysis, 23 proteins, FBL, Nop56, IMP4, MPHOSPH10 (Mpp10), Noc4L, Nop14, UTP3, RRP7A, Guα (DDX21), DDX51, PELP1, TEX10, WDR18, LAS1L, MDN1, NOL9, SENP3, Nop52, DDX54, DDX56, NO66, and RRP12-like protein, and Guβ (DDX50), are involved or expected to be involved in human ribosome biogenesis (Table I) (45–57). In addition, three nucleolar proteins (MYBBP1A, NOM1, and RRP1B), and five subunits of the general transcription factors (3C polypeptides 1–5) required for RNA polymerase III-dependent transcription, were also identified (Tables I and II).

To examine the possible involvement of p32 in ribosome biogenesis, we first performed an additional immunoblot analysis of the p32-FLAG-associated proteins with 10 available antibodies against Nop58, PM/Scl100, PWP1, RRP40, RRP46, FTSJ2, nucleolin (NCL), B23, and NOC2L as well as the catalytic component of RNA polymerase III RPC7, which are involved or probably involved in ribosome biogenesis but were not identified by the mass-based analyses. Six of the proteins (Nop58, PM/Scl100, FTSJ2, NCL, RRP40, and RPC7) were detected by the analysis (Fig. 1*D*, and Table I); those that were not detected are excluded from Fig. 1*D* (data not shown).

We next performed reverse pull-down analysis using Nop52, FBL, RNA helicases Guα and Guβ, and NCL, which are involved in ribosome biogenesis, as affinity bait to examine their reciprocal associations with p32 with and without RNase treatment (Figs. 2*A*, 2*B*, 2*C*, and 2*D*). Nop52, FBL, Guα, and Guβ remained associated with p32 even after RNase treatment (Figs. 2*A*, 2*B*, and 2*C*), whereas NCL was associated with p32 only in the presence of RNA (Fig. 2*D*). Consistent with the proteomic analysis reported (26), FLAG-Nop52 did not associate with FBL, and FLAG-FBL did not associate with Nop52 (Fig. 2*A*). However, p32-FLAG associated with both FBL and Nop52 (Fig. 2*A*), suggesting that the association of p32 with FBL was independent of its association with Nop52.

FIG. 4. **The presence of p32 in the nucleolus/Cajal body fraction prepared by cell fractionation and in the preribosome fractions separated by ultracentrifugation.** Equivalent amounts of whole-cell extract (WCE), cytoplasmic fraction (Cyto), nucleoplasmic extract (NE), and nucleolar extract (NoE) prepared from 293EBNA cells transfected with (+) or without (–) a p32-specific siRNA (*A*), or transfected with (+) or without (–) p32-FLAG expression vector (*B*), were analyzed by immunoblotting with the antibodies indicated at the left. *C*, Cells were fractionated into nuclear (Nu) and cytoplasmic (Cyto) fractions and were analyzed by immunoblotting (IB) with the antibodies indicated (*left*, *top*). The Nu fraction that corresponded to the nuclear extract combining NE and NoE in (*A*) was separated on 10–30% sucrose density gradients and separated into 20 fractions. The absorbance at 254 nm was monitored and is shown on the top right. Proteins in each fraction were analyzed by immunoblotting with the antibodies indicated at the left (*middle*). RNAs were also extracted from each fraction, separated by agarose gel electrophoresis, transferred to a membrane, and stained with methylene blue (*bottom*). Input: 20 μg of protein from unfractionated Nu was loaded for immunoblotting; 2 μg of RNA from unfractionated Nu was loaded for agarose gel electrophoresis and methylene blue staining. *D*, Structure of the primary rRNA transcript (47S), outline of pre-rRNA processing in mammalian cells adapted from refs. 41, 52, 75, and oligonucleotide probes used for hybridization analysis are indicated. The main processing sites termed 1 to 6 correspond to the ends of mature 18S, 5.8S, and 28S rRNAs are also indicated. The external and internal transcribed spacers (ETS and ITS, respectively) contain additional cleavage sites designated A', A0, 2b, 2c, and 4b. *E*, RNAs extracted from p32-associated complex were detected by Northern blot analysis with the oligonucleotide probes indicated. Positions of pre-rRNAs and the probes used are indicated on the left and right, respectively. Input: 2 μg of RNA extracted from soluble cell lysates from control cells were loaded. Total RNA: 2 μg of total RNA were loaded. *F*, RNAs containing newly synthesized pre-rRNAs labeled with [^{3}H]uridine were isolated from p32-associated complex, separated on an agarose gel, transferred to a membrane, and detected by fluorography. Positions of pre-rRNAs are indicated on the left. Input: RNAs (5000 cpm/lane) extracted from soluble cell lysates were loaded.

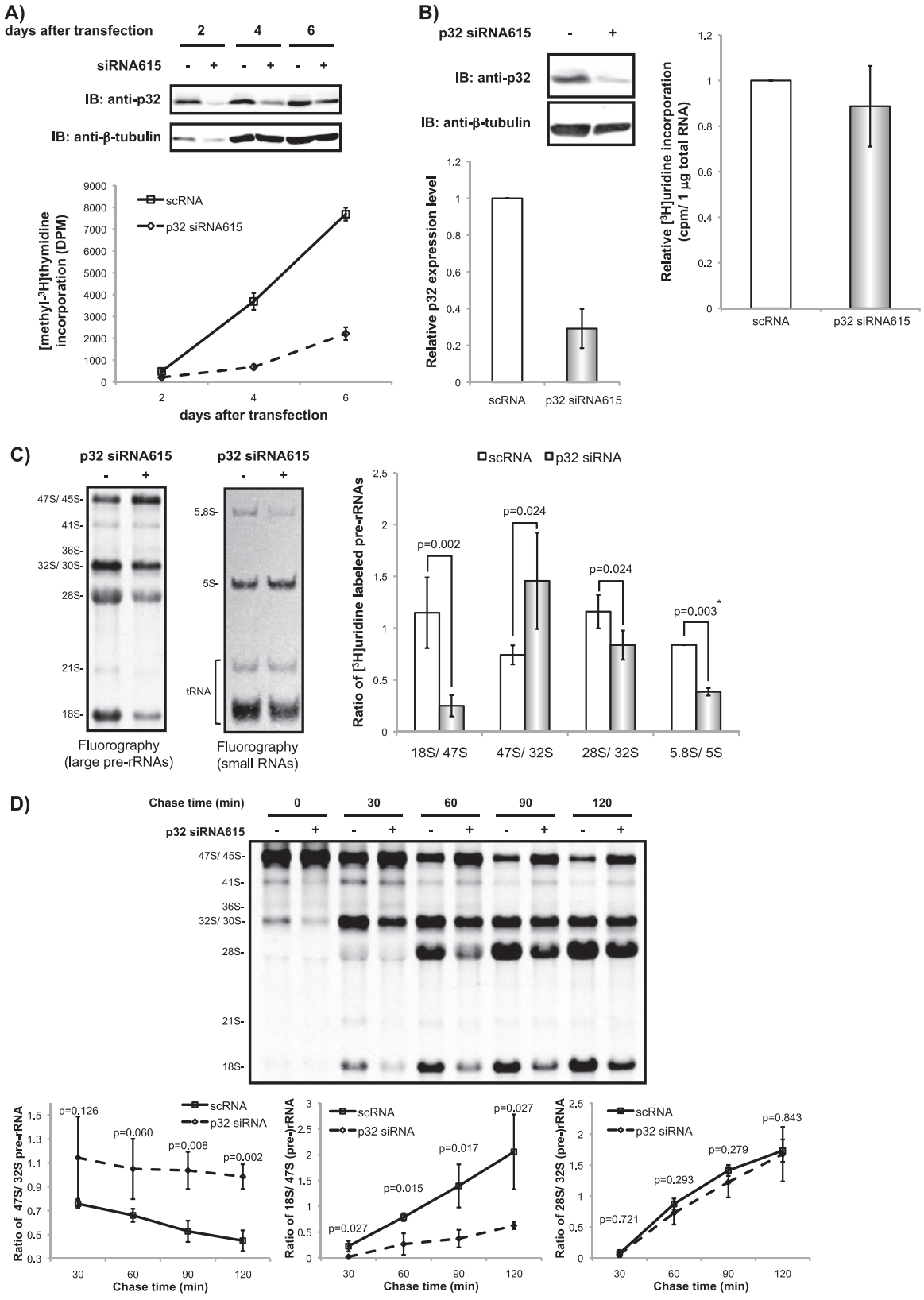
A)
days after transfection
2
4
6
siRNA615
- + - + - +
IB: anti-p32
IB: anti-β-tubulin
[methyl-3H]thymidine incorporation (DPM)
scRNA
p32 siRNA615
days after transfection
B)
p32 siRNA615
- +
IB: anti-p32
IB: anti-β-tubulin
Relative p32 expression level
scRNA
p32 siRNA615
Relative [3H]uridine incorporation (cpm/ 1 µg total RNA)
scRNA
p32 siRNA615
C)
p32 siRNA615
- +
47S/ 45S-
41S-
36S-
32S/ 30S-
28S-
21S-
18S-
Fluorography (large pre-rRNAs)
p32 siRNA615
- +
5.8S-
5S-
tRNA
Fluorography (small RNAs)
scRNA
p32 siRNA
Ratio of [3H]uridine labeled pre-rRNAs
p=0.002
p=0.024
p=0.024
p=0.003*
18S/ 47S
47S/ 32S
28S/ 32S
5.8S/ 5S
D)
Chase time (min)
0
30
60
90
120
p32 siRNA615
- + - + - + - + - +
47S/ 45S-
41S-
36S-
32S/ 30S-
28S-
21S-
18S-
Ratio of 47S/ 32S pre-rRNA
scRNA
p32 siRNA
p=0.126
p=0.060
p=0.008
p=0.002
Chase time (min)
Ratio of 18S/ 47S (pre-)rRNA
scRNA
p32 siRNA
p=0.027
p=0.015
p=0.017
p=0.027
Chase time (min)
Ratio of 28S/ 32S (pre-)rRNA
scRNA
p32 siRNA
p=0.721
p=0.293
p=0.279
p=0.843
Chase time (min)

p32 Is Localized in the Nucleolus and Is Present in Preribosomal Fractions—p32 is primarily localized in mitochondria and in the cytoplasm but can accumulate in the nucleus in response to leptomycin B or actinomycin D treatment of cells (58), whereas FBL and Nop52 are predominantly localized in the nucleoli during interphase (34). Therefore, we re-examined the localization of p32 in 293EBNA cells by immunocytochemical costaining. Although most p32 molecules were localized in mitochondria as reported (Fig. 3*A*, whole-cell view), they were dispersed as several minimum dots within the nucleus, some of which were present in high density and co-localized with FBL (Fig. 3*A*, nuclear view). By contrast, Nop52 was concentrated in the nucleolar periphery (Fig. 3*B*, nuclear view) and colocalized partly with p32. We also found that Nop52 co-localized with p80-coilin and that p32 colocalized with both p80-coilin and SMN, each of which is a marker of Cajal bodies (Figs. 3*C*, 3*D*, and 3*E*), suggesting that p32 and Nop52 also localize in Cajal bodies, as does FBL. In addition, upon treatment with actinomycin D, p32 was excluded from the nucleolus and was dispersed throughout the nucleoplasm in many dots (Fig. 3*F*), consistent with the relocalization of B23, a nucleolar marker that relocalizes to the nucleoplasm in response to actinomycin D (39); notably, the total amount of p32 in the cells was not affected (Fig. 3*G*). In concert, actinomycin D caused hyper-phosphorylation of the RNA polymerase II large subunit (Fig. 3*G*), as expected (59).

We also detected p32 in the nucleolar/Cajal body fraction (NoE) (Figs. 4*A* and 4*B*). siRNA treatment reduced the level of p32 in the NoE (Fig. 4*A*), whereas transfection of a p32-FLAG-encoded plasmid increased p32 in the NoE (Fig. 4*B*). These results indicate that the antibody we used specifically reacted with p32 and strongly suggest that p32 is present in the NoE. Furthermore, p32 coeluted with Nop52 and FBL in pre-60S fractions and fractions with higher sedimentation velocity separated by sucrose gradient ultracentrifugation of the Nu (Fig. 4*C*). This ultracentrifugation separated pre-60S particles from the pre-40S particles almost completely, as indicated by methylene blue staining of their rRNA components; namely, 18S rRNA was detected exclusively in the pre-40S fractions, whereas 28S and 32S rRNAs were detected only in pre-60S fractions (Fig. 4*C*). p32 was also detected with FBL, but not with Nop52, in the pre-40S fractions; however, p32 separation between pre-40S and pre-60S peaks is less clear than that of either FBL or Nop52 (Fig. 4*C*). The RNA helicases Guα and Guβ, whose association with p32 was independent of the presence of RNA (Figs. 2*B* and 2*C*), also coeluted with p32 in the pre-40S and pre-60S fractions (Fig. 4*C*). In addition, p32 associated at least with 47S, 45S, 41S, 32S, and 12S pre-rRNAs as detected by Northern blot analysis (Figs. 4*D* and 4*E*). 47S/45S and 32S/30S pre-rRNA were also detected in the p32-associated complex that was pulse-labeled with [^{3}H]uridine (Fig. 4*F*). Thus, p32 behaves *in vivo* as a component of preribosomal particles in all aspects that were examined.

p32 Is Involved in the Processing of pre-rRNA—To clarify the involvement of p32 in ribosome biogenesis, we examined the effects of RNAi-mediated p32 knockdown on the production of rRNAs. The knockdown of p32 mRNA level of the cell with the stealth p32 siRNA615 reduced the expression of the protein when compared with the control siRNA treated cells and suppressed significantly the cell growth as reported (60) (Fig. 5*A*). The p32 siRNA615 caused only a marginal reduction in cellular uptake of [^{3}H]uridine (Fig. 5*B*). The knockdown reduced significantly the production of 18S rRNA and 32S pre-rRNAs, whereas it accumulated 47S/45S pre-rRNA (Fig. 5*C*). Pulse-chase analysis using [^{3}H]uridine confirmed the reduction of the early processing of pre-rRNAs from 47S/45S to 18S rRNA and 32S pre-rRNA (Figs. 4*D* and 5*D*).

Nop52 Competes with FBL for Binding to p32—Given the result that the association of p32 with FBL was independent of its association with Nop52, we postulated that p32 was involved in ribosome biogenesis by mediating competitive binding of FBL and Nop52 to pre-ribosome particles. To first ascertain a direct association between Nop52 and p32, we constructed expression vectors for 19 FLAG-tagged-Nop52 truncated mutants to identify the region in Nop52 that was

FIG. 5. **Suppression of 47S/45S pre-rRNA processing by knockdown of p32.** *A*, Immunoblotting (IB) was used to determine the p32 expression level in the cells used for the proliferation assay. Whole-cell extracts prepared from cells transfected with scRNA (–) or p32 siRNA615 (+) were analyzed by immunoblotting with anti-p32 and anti-β-tubulin. The proliferation of siRNA615-transfected cells was monitored by measuring [methyl-^{3}H]Thymidine incorporation into DNA with Insta-Gel Plus. The *y* axis is shown as [^{3}H] incorporation disintegration per minute (DPM). The values indicated are averages (±S.D.) of six independent experiments. *B*, Immunoblotting was used to determine the p32 expression level in whole-cell extracts prepared from HeLa cells transfected with scRNA (–) or p32 siRNA615 (+) for 72 h. Newly synthesized RNA prepared from the cells transfected as in left was measured by [^{3}H]uridine incorporation into total RNA by scintillation counting (cpm) and normalized to 1 μg of total RNA. The values indicated are averages (±S.D.) of three independent experiments. *C*, RNA containing newly synthesized pre-rRNAs labeled with [^{3}H]uridine was isolated, and 20,000 cpm per sample were resolved on an agarose gel and transferred to a membrane (*left*) or on a polyacrylamide gel and transferred to a membrane (*middle*), and detected by fluorography. Positions of rRNAs are indicated on the left of each fluorogram. Ratio of labeled (pre-)rRNAs in each lane was compared between scRNA and siRNA615 treated cells. The values indicated in the graph are averages (±S.D.) of four independent experiments or two independent experiments (*). *p* values are also indicated in each comparison. *D*, Cells transfected as in (*B*) were pulse-labeled with [^{3}H]uridine for 30 min and cultured in nonradioactive medium for the time indicated. Total RNA (20,000 cpm/lane) was resolved on an agarose gel and transferred to a membrane and detected by fluorography (*upper left*). Positions of rRNAs and major precursors are indicated on the left of the picture. Ratio of 18S/47S (*lower left*), 47S/32S (*upper right*), or 28S/32S (*lower right*) in the staining intensity in the fluorography (*upper left*) is plotted against the times indicated. The values are averages (±S.D.) of three independent experiments.

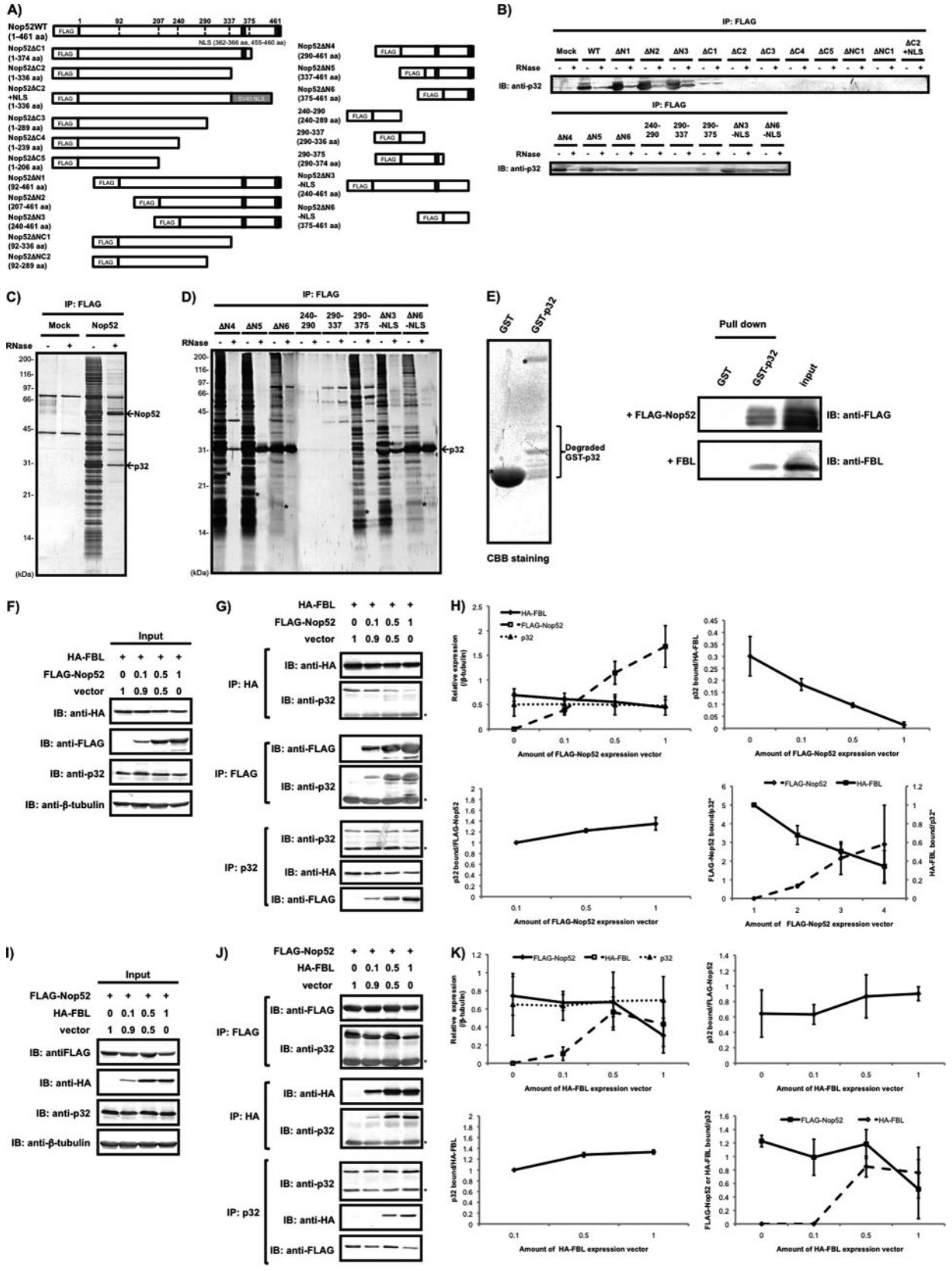
A)
Nop52WT (1-461 aa)
Nop52ΔC1 (1-374 aa)
Nop52ΔC2 (1-336 aa)
Nop52ΔC2 +NLS (1-336 aa)
Nop52ΔC3 (1-289 aa)
Nop52ΔC4 (1-239 aa)
Nop52ΔC5 (1-206 aa)
Nop52ΔN1 (92-461 aa)
Nop52ΔN2 (207-461 aa)
Nop52ΔN3 (240-461 aa)
Nop52ΔNC1 (92-336 aa)
Nop52ΔNC2 (92-289 aa)
Nop52ΔN4 (290-461 aa)
Nop52ΔN5 (337-461 aa)
Nop52ΔN6 (375-461 aa)
240-290 (240-289 aa)
290-337 (290-336 aa)
290-375 (290-374 aa)
Nop52ΔN3 -NLS (240-461 aa)
Nop52ΔN6 -NLS (375-461 aa)
B)
IP: FLAG
Mock WT ΔN1 ΔN2 ΔN3 ΔC1 ΔC2 ΔC3 ΔC4 ΔC5 ΔNC1 ΔNC1 ΔC2 +NLS
RNase
IB: anti-p32
ΔN4 ΔN5 ΔN6 240-290 290-337 290-375 ΔN3 -NLS ΔN6 -NLS
C)
IP: FLAG
Mock Nop52
Nop52
p32
D)
IP: FLAG
E)
GST GST-p32
Degraded GST-p32
CBB staining
Pull down
GST GST-p32 input
+ FLAG-Nop52
IB: anti-FLAG
+ FBL
IB: anti-FBL
F)
Input
HA-FBL
FLAG-Nop52
vector
IB: anti-HA
IB: anti-FLAG
IB: anti-p32
IB: anti-β-tubulin
G)
IP: HA
IP: FLAG
IP: p32
H)
HA-FBL
FLAG-Nop52
p32
Relative expression (/β-tubulin)
Amount of FLAG-Nop52 expression vector
p32 bound/HA-FBL
p32 bound/FLAG-Nop52
FLAG-Nop52 bound/p32*
HA-FBL bound/p32*
I)
Input
FLAG-Nop52
HA-FBL
vector
IB: antiFLAG
IB: anti-HA
IB: anti-p32
IB: anti-β-tubulin
J)
IP: FLAG
IP: HA
IP: p32
K)
FLAG-Nop52
HA-FBL
p32
Relative expression (/β-tubulin)
Amount of HA-FBL expression vector
p32 bound/FLAG-Nop52
p32 bound/HA-FBL
FLAG-Nop52 or HA-FBL bound/p32

responsible for binding to p32 (Fig. 6*A*). These truncated mutants were constructed based on the exon-intron boundaries of the Nop52 gene, the domain structure, and the presence of two probable nuclear localization signals at the C-terminal region of Nop52 (http://www.ncbi.nlm.nih.gov/sites/entrez?Db = gene&Cmd = retrieve&dopt = full_reporttwo nuc&list_uids = 8568&log$ = databasead&logdbfrom = nuccore#refseq). The expression and cellular localization of the truncated proteins were examined by SDS-PAGE and immunocytochemistry, respectively (supplemental Fig. S2A and S2B). All truncated mutants were expressed in the cell (supplemental Fig. S2B) and showed the expected molecular sizes as estimated from their amino acid sequences, with the exception of mutant 240–290, which was detected by immunocytochemical analysis but not by the SDS-PAGE (supplemental Fig. S2A). Immunoblotting with anti-p32 showed that domain mutants Nop52ΔN1, ΔN2, ΔN3, ΔN4, ΔN5, and ΔN6 were associated with p32 (Fig. 6*B*). In addition, Nop52ΔN3 and ΔN6 mutants lacking the C-terminal NLS (Nop52ΔN3-NLS and Nop52ΔN6-NLS) also associated with p32 (Fig. 6*B*). All of these mutants primarily localized in the nucleolus (supplemental Fig. S2B), suggesting that the interaction between Nop52 and p32 occurs in the nucleolus. On the other hand, all other mutants lacking the region 375–454 (except Nop52ΔC1 and Nop52 290–375) did not associate with p32 (Fig. 6*B*). These results clearly indicate that the minimal region of Nop52 corresponding to ΔN6-NLS (375–454) is sufficient to interact with p32. Silver staining of SDS-PAGE gels showed that the ΔN5, ΔN6, and ΔN6-NLS mutants were associated almost exclusively with p32 after RNase treatment, whereas wild-type Nop52 associated with several proteins, including p32, independently of the presence of RNA (Figs. 6*C* and 6*D*). To examine further the direct interaction between p32 and Nop52, we synthesized recombinant GST-p32 and GST-thrombin cleavage site-FLAG-Nop52 using *E. coli* DL21 and isolated GST-p32 by affinity chromatography and FLAG-Nop52 by thrombin cleavage from GST-thrombin cleavage site-FLAG-Nop52 bound glutathione-fixed beads (39). We mixed the isolated GST-p32 with FLAG-Nop52, pulled down with glutathione-fixed beads, and confirmed the interaction between GST-p32 and FLAG-Nop52 by immunoblotting with anti-FLAG antibody (Fig. 6E). These results indicate that Nop52 associates directly with p32 at the C-terminal region of Nop52 and that the binding does not require cofactors.

To examine the possible competition between FBL and Nop52 for binding to p32, we transfected the HA-FBL plasmid with a mixture of pcDNA3.1 vector and FLAG-Nop52 plasmid at different ratios, pulled down proteins with anti-HA, anti-FLAG, or anti-p32 immobilized on beads, and detected p32, HA-FBL, or FLAG-Nop52 among the pulled-down proteins by immunoblotting. The expression of FLAG-Nop52 reduced FBL-associated p32 in a dose-dependent manner, whereas the amount of Nop52-associated p32 increased with an increase in Nop52 expression (Figs. 6F-6H). In addition, p32-associated HA-FBL decreased with an increased association of FLAG-Nop52 in the protein complex isolated with anti-p32 antibody (Figs. 6*G* and 6*H*). On the other hand, when the

FIG. 6. **Competitive binding of FBL and Nop52 to p32.** *A*, Schematic representation of FLAG-tagged wild-type Nop52 (WT) and its truncation mutants used in this study. Abbreviations used are indicated in the text. Proteins were immunoprecipitated (IP) with anti-FLAG from whole-cell extracts of 293EBNA cells transfected with FLAG-Nop52 or its truncation mutants (see text for descriptions) and detected by immunoblotting (IB) with anti-p32 before (–) and after (+) treatment with RNase A (*B*) or by silver staining of a 12% SDS-PAGE gel (*C*, FLAG-Nop52; *D*, its truncation mutants). Asterisk indicates the position of its corresponding domain mutant migrated. The *arrows* indicate p32 and FLAG-Nop52 (Nop52). *E*,The isolated GST-p32 or GST was mixed with purified FLAG-Nop52 or FBL, pulled down with glutathione-fixed beads, and detected by immunoblotting with anti-FLAG antibody or anti-FBL antibody. The CBB-stained SDS-PAGE gel showed that the used-GST-p32 contained several degraded fragments that were detected by immunoblotting with anti-GST antibody (Degraded GST-p32). The isolated FLAG-Nop52 had several forms that were probably produced during thrombin cleavage (see *Materials and Methods*). (*F*, *G*) The expression vector encoding FLAG-Nop52 was mixed with pcDNA3.1(+) empty vector in the ratios indicated and then cotransfected with a constant amount of the HA-FBL expression vector. HA-FBL, FLAG-Nop52, p32 or β-tubulin was detected by immunoblotting with the corresponding antibodies in the cell extract (input) (*F*) or in the complex isolated by immunoprecipitation with anti-HA, anti-FLAG, or anti-p32 from the co-transfected cells (*G*). Asterisks in *F* and *G* indicate the light chain of the antibody detected by immunoblotting. (*H*) Statistical evaluation of the results obtained in Figs. 6*F* and 6*G*. The horizontal axis is shown as the amount of FLAG-Nop52 expression vector mixed. Vertical axis is shown as: each protein expression detected with the indicated antibody shown in Fig. 6*F* is normalized by that of β-tubulin in the same lane (*upper left*); p32 bound/HA-FBL, amount of p32 bound to HA-FBL shown in Fig. 6*G* (IP:HA) is divided by that of HA-FBL (*upper right*); p32 bound/FLAG-Nop52, amount of p32 bound to FLAG-Nop52 shown in Fig. 6*G* (IP:FLAG) is divided by that of FLAG-Nop52 (*lower left*); FLAG-Nop52 bound/p32, amount of FLAG-Nop52 bound to p32 shown in Fig. 6*G* (IP:p32) is divided by that of p32, vertical axis right-amount of HA-FBL bound to p32 is divided by that of p32 (IP:p32) (*lower right*). The values indicated in the graph are averages (±S.D.) of three independent experiments or two independent experiments (*). (*I*, *J*) Transfection and immunoprecipitation of the mixture of the HA-FBL expression vector and pcDNA3.1(+) empty vector in different ratios over a constant amount of the FLAG-Nop52 expression vector was also performed. Asterisks in *I* and *J* indicate the light chain of the antibody detected by immunoblotting. (*K*) Statistical evaluation of the results obtained in Figs. 6*I* and 6*J*. The horizontal axis is shown as the amount of HA-FBL expression vector mixed. Vertical axis is shown as: each protein expression detected with the indicated antibody shown in Fig. 6*I* is normalized by that of β-tubulin in the same lane (*upper left*); p32 bound/FLAG-Nop52, amount of p32 bound to FLAG-Nop52 shown in Fig. 6*J* (IP:FLAG) is divided by that of FLAG-Nop52 (*upper right*); p32 bound/HA-FBL, amount of p32 bound to HA-FBL shown in Fig. 6*J* (IP:HA) is divided by that of HA-FBL *(lower left*,); FLAG-Nop52 or HA-FBLbound/p32, amount of FLAG-Nop52 or HA-FBL bound to p32 shown in Fig. 6*J* (IP:p32) is divided by that of p32 (*lower right*). The values indicated in the graph are averages (±S.D.) of three independent experiments.

expression of HA-FBL was increased whereas Nop52 expression remained constant, the amount of FBL-associated p32 increased some extent with an increase in FBL expression (Figs. 6*I*–6*K*); however, the decrease of the amount of FLAG-Nop52-associated p32 was not as evident as that of the amount of HA-FBL-associated p32 when the expression of FLAG-Nop52 was increased whereas FBL expression remained constant (Figs. 6*F*–6*K*). These results suggest that Nop52, but not the other way can replace FBL bound to p32.

The Association of FBL with p32 Takes Place in the Nucleolus—We next examined where in the cell the competition between FBL and Nop52 for binding to p32 takes place. We first used two FBL mutants that localized predominantly in the cytoplasm: Gly-Ala (GA) at residues 167–168 and Ala-Ala (AA) at residues 168–169 were replaced by Tyr-Tyr (YY; Y1) and Trp-Tyr (WY; W2), respectively (supplemental Fig. 3A and 3B). Each of the two mutants was able to associate with p32 in whole-cell extracts (Fig. 7*A*, WCE); however, wild-type FBL or the mutants did not associate with p32 in the cytoplasmic fraction. On the other hand, wild-type FBL associated with p32 in the nuclear fraction (Fig. 7*A*, Nu), indicating that the interaction between p32 and FBL takes place in the nucleus. As a reference, we also examined co-precipitation with PRMT1, PRMT5, and HSP70, which associate with FBL, and found that wild-type FBL associated with PRMT1 in both the nucleus and the cytoplasm, whereas it associated with PRMT5 and HSP70 only in the cytoplasm (Fig. 7*A*). Next we used two domain mutants without a NLS fusion—FBL-I corresponding to the GAR domain (residues 1–77), and FBL-II corresponding to the spacer region 1 (residues 78–132)—which were excluded from the nucleolus and localized in the nucleoplasm and the cytoplasm, respectively (supplemental Figs. S3C and S3D). We found that neither mutant associated with p32 (Fig. 7*B*). We observed that the expressed FBL-I had a molecular weight two fold greater than that predicted from its amino acid sequence; however, at present we do not know the cause of this discrepancy. However, when the NLS was fused to these mutants, they localized in the nucleolus but not in Cajal bodies (supplemental Figs. S3C and S3D), and they were able to associate with p32 (Fig. 7*B*) (26). These results suggest that nucleolar localization is required for the association of FBL with p32, and imply that p32 changes its interaction partner from FBL to Nop52 in the nucleolus.

p32 Is Associated with Nop52 in Pre-60S Particles—To confirm further the association of p32 with pre-60S particle, we used the pull-down method to isolate FLAG-Nop52-associated pre-60S particles from pre-60S fractions separated by sucrose gradient ultracentrifugation of the Nu (Figs. 8*A* and 8*B*). Immunoblotting with anti-p32 unambiguously detected p32 in isolated FLAG-Nop52-associated pre-60S particles (Fig. 8*C*). Thus, p32 is recruited indeed to Nop52-associated pre-60S ribosomal particles.

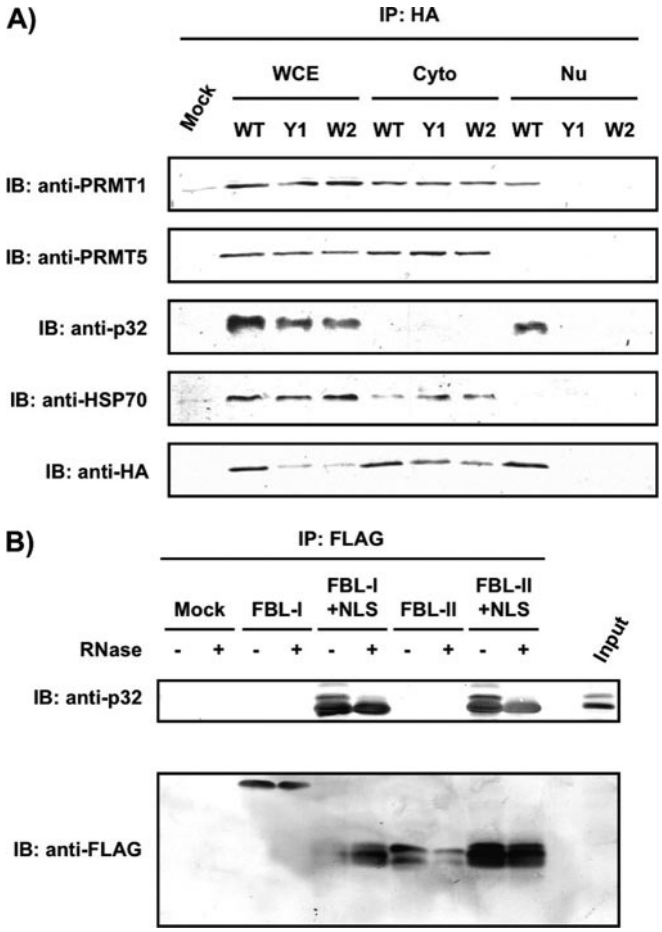

FIG. 7. **The association of FBL with p32 takes place in the nucleolus.** *A*, Proteins were immunoprecipitated (IP) with anti-HA from whole-cell extract (WCE), cytoplasmic fraction (Cyto), and nuclear fraction (Nu), which were prepared from 293EBNA cells transfected with an expression vector encoding HA-FBL, HA-Y1, or HA-W2. They were analyzed by immunoblotting (IB) with the antibodies indicated at the left. *B*, FLAG-FBL truncation mutant-associated protein complexes were immunoprecipitated with anti-FLAG after expression of various truncation mutants (FBL-I, FBL-I+NLS, FBL-II, or FBL-II+NLS) in 293EBNA cells, and analyzed by immunoblotting with anti-p32 before (–) and after (+) treatment with RNase A. Input: 30 μg of an aliquot of whole-cell extract was loaded.

DISCUSSION

In this study, we showed that 1) p32 associates with 31 proteins known or expected to be involved in rRNA processing (of which 10 proteins are classified as components of pre-90S particle, and 11 proteins as pre-60S particle, Table I), at least four of which are found to associate independently with p32; 2) p32 colocalizes with FBL or Nop52 in the nucleolus and is excluded from the nucleolus upon inhibition of transcription with actinomycin D; 3) p32 is present in the preribosomal fraction prepared by cell fractionation; 4) p32 coelutes with FBL or Nop52 in the pre-ribosomal fractions separated by ultracentrifugation; 5) p32 associates with pre-rRNAs, 6) p32 is present in the isolated Nop52-associated

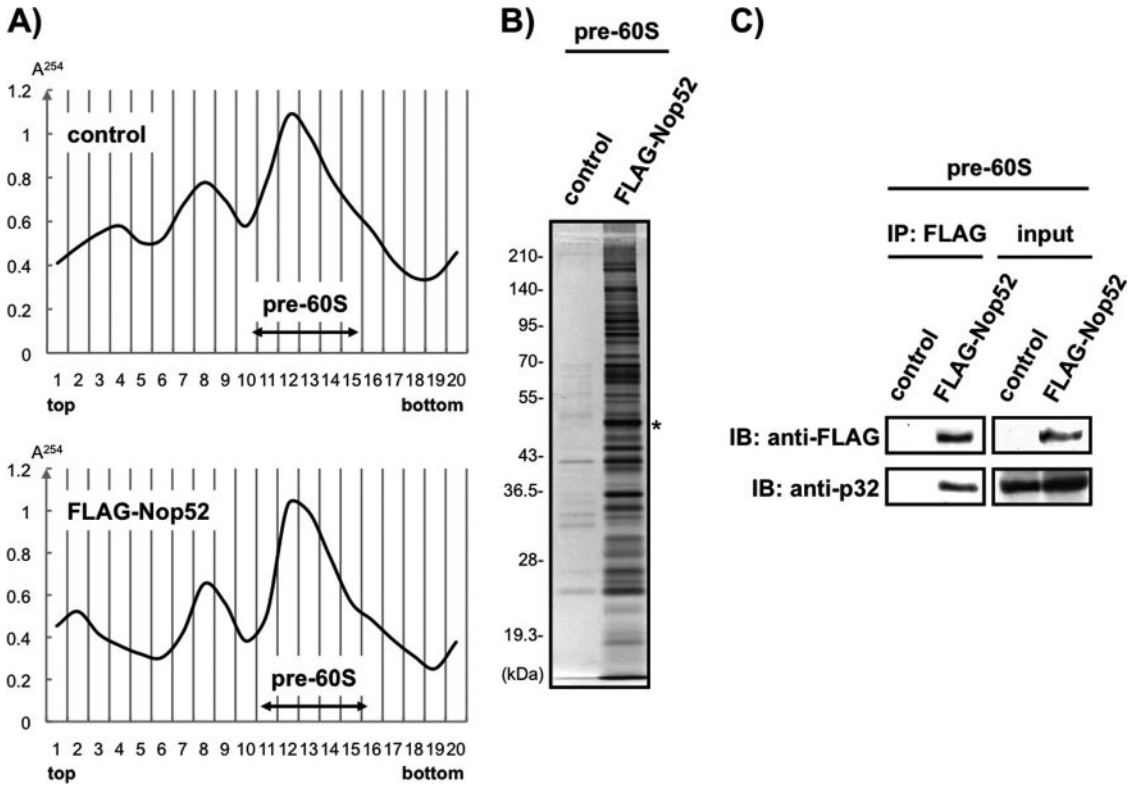

FIG. 8. **p32 is present in the Nop52-associated pre-60S particles.** *A*, The nuclear fraction prepared from control cells (control) that stably expressed hygromycin-resistant protein constructed by the transfection of pcDNA5/FRT/TO vector into Flp-In T-REx 293 cells or the inducible FLAG-Nop52 expression cells (FLAG-Nop52) was separated into 20 fractions by sucrose gradient ultracentrifugation. The absorbance at 254 nm was monitored to generate the profile indicated. The pre-60S fractions 11–15 were combined for each of the profiles independently and used for immunoprecipitation with anti-FLAG-fixed beads. *B*, The isolated proteins were analyzed by 10% SDS-PAGE and visualized by silver staining. Asterisk indicates FLAG-Nop52 as bait. The molecular masses (kDa) are indicated at the left. *C*, Association of p32 with Nop52 in isolated pre-60S ribosomal particles was confirmed by immunoblot (IB) analysis with anti-p32. An aliquot (5%) of the pre-60S combined fractions prepared from control or FLAG-Nop52 was used as input. IP: Immunoprecipitation.

pre-60S ribosomal particles; and 7) p32 knockdown slows down the early processing of pre-rRNAs. We conclude that p32 is a *de facto* component of pre-ribosomal particles and is involved in early nucleolar steps of ribosome biogenesis.

Our hypothesis for p32 involvement in ribosome biogenesis is that p32 exchanges its binding partner, *i.e.* p32 binds Nop52 in place of FBL, in preribosomal particles in the nucleolus. The p32-Nop52 complex then mediates transformation of FBL-associated pre-90S ribosomal particles formed in the dense fibrillar component (DFC) to Nop52-associated pre-60S ribosomal particles in the granular component (GC). This hypothesis is based on our results that 1) p32 association with Nop52 is independent of that with FBL; 2) p32 interacts with Nop52 without any cofactors, just as with FBL; 3) the association between FBL and p32 takes place in the nucleolus; 4) the association between Nop52 and p32 possibly occurs in the nucleolus, too; 5) p32 is required for the early processing of pre-rRNA from 47S/45S pre-rRNA to 18S rRNA and 32S pre-rRNA, 6) p32 associates with pre-rRNAs including 47S/45S and 32S pre-rRNAs, 7) p32 is present in Nop52-associated pre-60S ribosomal particles isolated from the nucleus; and 8) Nop52 competes with FBL for association with p32. We previously demonstrated that FBL associates with U3 snoRNP components (Nop56, Nop58, and a 15.5-kDa protein) and at least 27 pre-rRNA processing factors, but not with Nop52 (26, 57); we proposed that FBL functions in the pre-ribosomal particles formed from the early to middle stages of human ribosome biogenesis (26, 42, 61). We have also used mass-based proteomics to examine the constituents of the Nop52-associated preribosomal particles and identified 20 proteins involved or expected to be involved in ribosome biogenesis, but did not detect FBL as well as the other U3 snoRNP components (42, 62). These results indicate that FBL-associated preribosomal particles are distinct from those associated with Nop52. It is well established that FBL and Nop52 are involved in different stages of ribosome biogenesis in the nucleolus; FBL participates in early processing of rRNA, *i.e.* the processing of the 5′-external transcribed spacer, and localizes in the nucleolar DFC (46, 47, 63), whereas Nop52 is associated with late events related to the production of 60S ribosomal particle and localizes in the nucleolar GC (33–35). These observations support our hypothesis.

We propose two scenarios for this hypothesis. In the first scenario, p32 associates with pre-90S ribosomal particles formed in the early stages of ribosome biogenesis through FBL in the DFC. Subsequently, Nop52 targets p32 on the FBL-associated pre-90S ribosomal particles, thereby replacing FBL and initiating the formation of Nop52-associated pre-60S ribosomal particles, which accelerates the maturation of 28S rRNA in the later stages of ribosome biogenesis in the GC. In this scenario, preribosomal particles formed in the early stages would contain not only FBL but also p32. In fact, p32 was detected in fractions with a sedimentation coefficient larger than 60S (*i.e.* fractions 16–20 in Fig. 4*C*) and was associated with at least 10 proteins classified as components of pre-90S particle (Table I) as well as 47S/45S pre-rRNA (Figs. 4*E* and 4*F*). The presence of Nop52 in these fractions may indicate a transient preribosomal complex containing FBL, p32, and Nop52. This transit complex may be unstable and difficult to be isolated by the pull-down method we used. As p32 forms trimer with a doughnut-shaped quaternary structure with an unusually asymmetric charge distribution on the surface (64), it is possible that p32 acts as a bridge between FBL and Nop52 on the transient pre-ribosomal complex. After this exchange event, the Nop52-p32 complex in pre-60S ribosomal particle accelerates the processing of 32S pre-rRNA to 28S rRNA. The fact that one molecule of FBL binds to two molecules of p32—one in the GAR domain and another in spacer region 1 (26)—may explain the presence of p32 in FBL-associated pre-40S ribosome particles as well; *i.e.* only one of the p32 molecules is involved in competitive binding with Nop52, leaving the other p32 molecule associated with FBL in pre-40S ribosomal particles after the remodeling of preribosomal particles.

In the second scenario, FBL and Nop52 are both associated with preribosomal particles in a small population formed at a certain point in the early stages of ribosome biogenesis, but these intermediate preribosomal particles associated with FBL and Nop52 may be too unstable to isolate by the pull-down method. Then, a posttranslational modification of p32 and/or other proteins, or perhaps the entry of p32 and/or another protein(s) into the nucleolus, triggers remodeling of the FBL-Nop52-associated preribosomal particles to FBL-p32- and Nop52-p32-associated preribosomal particles formed at later stages of ribosome biogenesis. This scenario can also explain some of our results (*i.e.* Fig. 4, Fig. 5, and Fig. 8), such that p32 was required for the early processing of 47S/45S pre-rRNA, and that it was detected in pre-40S and pre-60S particles and in fractions with a sedimentation coefficient larger than 60S fractions. Both scenarios suggest that p32 is required to distinguish Nop52-associated pre-60S ribosomal particles from those associated with FBL. p32 may function to validate the proper assembly of FBL-associated pre-90S ribosomal particles formed at early stages of ribosome biogenesis before carrying out processes such as the cleavage of the internal transcribed spacer 2 in Nop52-associated pre-60S ribosomal particles at later stages.

We also detected p32, FBL, and Nop52 in fractions with sedimentation velocity smaller than 40S separated by sucrose gradient ultracentrifugation (Fig. 4*C*). Although no direct evidence for the involvement of these protein populations in ribosome biogenesis is currently available, the relative amounts and interactions among these proteins may determine the supply of each protein to the sites of ribosome biogenesis. In this context, their localization in Cajal bodies may be related to a mechanism underlying this level of regulation.

It has been reported that yeast Mam33p (mitochondrial acidic matrix protein) and the putative *Caenorhabditis elegans* gene product F59A-2.3 are functional homologs of human p32 (65). The two homologs are synthesized as precursors with an N-terminal mitochondrial targeting sequence that is cleaved upon import, and they are located mainly in mitochondria. Those proteins also have conserved structural features, including the prevalence of acidic amino acids and the occurrence in homo-oligomeric complexes (64). To re-examine possible evolutionary conservation of the p32 amino acid sequence in organisms lower than yeast (prokaryotic organisms), we searched for protein sequences that align with the entire human p32 sequence (UniProt: C1QBP_HUMAN) in the database containing nonfragmented sequences of bacteria (5,338,921 entries) and archaebacteria (182,058 entries) extracted from UniProt (SwissProt, release 57.4 and TrEMBL, release 40.4) using BlastP (*E*-value < 0.1 with SEG filtering) and PSI-BLAST (*E*-value < 0.1, 10 iterations). No homologs were detected by PSI-BLAST, and only one hit, B8K7P_VIBPA, was found by BlastP. Although this protein has 28% sequence identity with human p32, it is unlikely to be a functional homolog, as it has neither the sequence motif (Pfam02330) nor the structural unit (SCOP d.25.1.1) of human p32 (64), which adopts a novel fold with seven consecutive anti-parallel β-strands flanked by one N-terminal and two C-terminal α-helices. By contrast, yeast homologs of human p32, MAM33_YEAST (*Saccharomyces cerevisiae*) and MAM33_SCHPO (*Schizosaccharomyces pombe*) were identified as homologs of human p32 at *E*-values < 0.1 by BlastP and PSI-BLAST, and both have Pfam02330 and SCOP d.25.1.1 domains. These results suggest that p32 evolved in eukaryotes rather than prokaryotes. Although the involvement of Mam33p in ribosome biogenesis has not been reported, large-scale proteomic analyses have demonstrated that Mam33p associates with Nop7p and Mrt4p, which are involved in rRNA processing and are components of yeast pre-66S ribosome particles (66, 67). By large-scale proteomic analyses Mam33p was also shown to be associated with several mitochondrial ribosome proteins in yeast (67). Thus, it is likely that the involvement of p32 in ribosome biogenesis is conserved among eukaryotes from yeast to human. However, Mam33p may be involved in ribosome biogenesis by a mech-

anism different from that in humans, as yeast Rrp1p does not have much sequence similarity in the region of Nop52 that binds to p32 (33).

p32 also interacts with herpes simplex virus 1 Orf-P protein (17), HIV-1 Tat (24), and Epstein-Barr virus EBNA 1 protein (20). Ribosomal proteins are synthesized up to the late stage of herpes simplex virus 1 infection and efficiently assemble into mature ribosomes, whereas there is a severe shutoff of the synthesis of other cellular proteins (68). Upon infection, this virus also alters the nuclear transport of preribosomal particles (69). In the case of HIV1, Tat protein affects processing of pre-rRNA, probably through the interaction with FBL (70). Regarding Epstein-Barr virus, the yeast homolog of EBNA1-binding protein is essential for biogenesis of the 60S subunit (71). These reports suggest that these virus proteins influence ribosome biogenesis by interrupting or modifying the interaction of p32 with FBL or Nop52. It has also been established that several viruses and viral proteins enter the nucleolus; viral proteins co-localize with factors such as nucleolin, B23, and FBL, and can cause their redistribution during infection (72, 73). In the case of hepatitis C virus, its infection even modifies transcription of rDNA (74); thus, the nucleolar processes of ribosome biogenesis seem to be common targets for viral infection. As such, a more detailed understanding of viral protein interactions with the ribosome-generating machinery may lead to novel antiviral therapies.

Acknowledgments—We would like to express our deepest condolences to the death of Miss Miyuki Kawasaki who initiated this study, and thank Dr. D. Hernandez-Verdun for the generous gift of human anti-Nop52 (NNP1), Dr. A. R. Krainer for mouse monoclonal anti-p32, and Dr. W. C. Russell for rabbit polyclonal anti-p32.

* This work was supported in part by a grant for promotion from the Ministry of Education, Culture, Sports, Science, and Technology of Japan (MEXT), the Japan Health Science Foundation (H18-Soyaku-Ippan-001), the Core Research for Evolutional Science and Technology (CREST), Japan Science and Technology Agency (JST), and the Targeted Proteins Research Program (TPRP) from the MEXT.

S This article contains supplemental Figs. S1 to S3 and Tables S1 and S2.

[a] To whom correspondence should be addressed: Applied Biological Science, Tokyo University of Agriculture and Technology, 3-5-8 Saiwai-cho, Fuchu, Tokyo 183-8509, Japan. Fax No.+81-042-367-5709; E-mail: ntakahas@cc.tuat.ac.jp.

REFERENCES

1. Krainer, A. R., Mayeda, A., Kozak, D., and Binns, G. (1991) Functional expression of cloned human splicing factor SF2: homology to RNA binding protein VI 70K, and *Drosophila* splicing regulators. *Cell* **66,** 383–394
2. Petersen-Mahrt, S. K., Estmer, C., Ohrmalm, C., Matthews, D. A., Russell, W. C., and Akusjävi, G. (1999) The splicing factor-associated protein, p32, regulates RNA splicing by inhibiting ASF/SF2 RNA binding and phosphorylation. *EMBO J.* **18,** 1014–1024
3. Mayeda, A., and Krainer, A. R. (1992) Regulation of alternative pre-mRNA splicing by hnRNP A1 and splicing factor SF2. *Cell* **68,** 365–375
4. Mayeda, A., Helfman, D. M., and Krainer, A. R. (1993) Modulation of exon skipping and inclusion by heterogeneous nuclear ribonucleoprotein-A1 and premessenger RNA splicing factor SF2/ASF. *Mol. Cell. Biol.* **13,** 2993–3001
5. Sun, Q., Mayeda, A., Hampson, R. K., Krainer, A. R., and Rottman, F. M. (1993) General splicing factor SF2/ASF promotes alternative splicing by binding to an exonic splicing enhancer. *Genes Dev.* **7,** 2598–2608
6. Yang, X., Bani, M. R., Lu, S. J., Rowan, S., Ben-David, Y., and Chabot, B. (1994) The A1 and A1B proteins of heterogeneous nuclear ribonucleoparticles modulate 5′ splice site selection *in vivo*. *Proc. Natl. Acad. Sci. U.S.A.* **91,** 6924–6928
7. Chabot, B., Blanchette, M., Lapierre, I., and La Branche, H. (1997) An intron element modulating 5′ splice site selection in the hnRNP A1 pre-mRNA interacts with hnRNP A1. *Mol. Cell. Biol.* **17,** 1776–1786
8. Hanamura, A., Cáceres, J. F., Mayeda, A., Franza, B. R., Jr., and Krainer, A. R. (1998) Regulated tissue-specific expression of antagonistic pre-mRNA splicing factors. *RNA* **4,** 430–444
9. Jiang, Z. H., Zhang, W. J., Rao, Y., and Wu, J. Y. (1998) Regulation of Ich-1 pre-mRNA alternative splicing and apoptosis by mammalian splicing factors. *Proc. Natl. Acad. Sci. U.S.A.* **95,** 9155–9160
10. Ghebrehiwet, B., Lim, B. L., Peerschke, E. I., Willis, A. C., and Reid, K. B. (1994) Isolation, cDNA cloning, and overexpression of a 33-kD cell surface glycoprotein that binds to the globular 'heads' of C1q. *J. Exp. Med.* **179,** 1809–1821
11. Yadav, G., Prasad, R. L., Jha, B. K., Rai, V., Bhakuni, V., and Datta, K. (2009) Evidence for inhibitory interaction of hyaluronan-binding protein 1 (HABP1/p32/gC1qR) with *Streptococcus pneumoniae* hyaluronidase. *J. Biol. Chem.* **284,** 3897–3905
12. Deb, T. B., and Datta, K. (1996) Molecular cloning of human fibroblast hyaluronic acid-binding protein confirms its identity with P-32, a protein co-purified with splicing factor SF2. Hyaluronic acid-binding protein as P-32 protein, co-purified with splicing factor SF2. *J. Biol. Chem.* **271,** 2206–2212
13. Chattopadhyay, C., Hawke, D., Kobayashi, R., and Maity, S. N. (2004) Human p32, interacts with B subunit of the CCAAT-binding factor, CBF/NF-Y, and inhibits CBF-mediated transcription activation in vitro. *Nucleic Acids Res.* **32,** 3632–3641
14. Itahana, K., and Zhang, Y. (2008) Mitochondrial p32 Is a Critical Mediator of ARF-Induced Apoptosis. *Cancer Cell* **13,** 542–553
15. Sunayama, J., Ando, Y., Itoh, N., Tomiyama, A., Sakurada, K., Sugiyama, A., Kang, D., Tashiro, F., Gotoh, Y., Kuchino, Y., and Kitanaka, C. (2004) Physical and functional interaction between BH3-only protein Hrk and mitochondrial pore-forming protein p32. *Cell Death Differ.* **11,** 771–781
16. Simos, G., and Georgatos, S. D. (1994) The lamin B receptor-associated protein p34 shares sequence homology and antigenic determinants with the splicing factor 2-associated protein p32. *FEBS Lett.* **346,** 225–228
17. Bruni, R., and Roizman, B. (1996) Open reading frame P-a herpes simplex virus gene repressed during productive infection encodes a protein that binds a splicing factor and reduces synthesis of viral proteins made from spliced mRNA. *Proc. Natl. Acad. Sci. U.S.A.* **93,** 10423–10427
18. Matthews, D. A., and Russell, W. C. (1998) Adenovirus core protein V interacts with p32-a protein, which is associated with both the mitochondria and the nucleus. *J. Gen. Virol.* **79,** 1677–1685
19. Wang, Y., Finan, J. E., Middeldrop, J. M., and Hayward, S. D. (1997) p32/TAP, a cellular protein that interacts with EBNA-1 of Epstein-Barr virus. *Virology* **236,** 18–29
20. Chen, M. R., Yang, J. F., Wu, C. W., Middeldorp, J. M., and Chen, J. Y. (1998) Physical association between the EBV protein EBNA-1 and p32/TAP/hyaluronectin. *J. Biomed. Sci.* **5,** 173–179
21. Beatch, M. D., and Hobman, T. C. (2000) Rubella virus capsid associates with host cell protein p32 and localizes to mitochondria. *J. Virol.* **74,** 5569–5576
22. Luo, Y., Yu, H., and Peterlin, B. M. (1994) Cellular protein modulates effects of human immunodeficiency virus type 1 Rev. *J. Virol.* **68,** 3850–3856
23. Tange, T. O., Jensen, T. H., and Kjems, J. (1996) In vitro interaction between human immunodeficiency virus type 1 rev protein and splicing factor ASF/SF2-associated protein p32. *J. Biol. Chem.* **271,** 10066–10072
24. Yu, L., Loewenstein, P. M., Zhang, Z., and Green, M. (1995) In vitro interaction of the human immunodeficiency virus type 1 Tat transactivator and the general transcription factor TFIIB with the cellular protein TAP. *J. Virol.* **69,** 3017–3023
25. Zheng, Y. H., Yu, H. F., and Peterlin, B. M. (2003) Human p32 protein relieves a post-transcriptional block to HIV replication in murine cells. *Nat. Cell Biol.* **5,** 611–618

26. Yanagida, M., Hayano, T., Yamauchi, Y., Shinkawa, T., Natsume, T., Isobe, T., and Takahashi, N. (2004) Human fibrillarin forms a sub-complex with splicing factor 2 associated p32, protein/arginine methyltransferases, tubulin α3 and β1, which is Independent of its association with preribosomal ribonucleoprotein complexes. *J. Biol. Chem.* **279,** 1607–1614
27. Warner, J. R. (1990) The nucleolus and ribosome formation. *Curr. Opin. Cell Biol.* **2,** 521–527
28. Kiss-László, Z., Henry, Y., Bachellerie, J. P., Caizergues-Ferrer, M., and Kiss, T. (1996) Site-specific ribose methylation of preribosomal RNA: a novel function for small nucleolar RNAs. *Cell* **85,** 1077–1088
29. Tycowski, K. T., Smith, C. M., Shu, M. D., and Steitz, J. A. (1996) A small nucleolar RNA requirement for site-specific ribose methylation of rRNA in *Xenopus. Proc. Natl. Acad. Sci. U.S.A.* **93,** 14480–14485
30. Tyc, K., and Steitz, J. A. (1989) U3, U8 and U13 comprise a new class of mammalian snRNPs localized in the cell nucleolus. *EMBO J.* **8,** 3113–3119
31. Baserga, S. J., Yang, X. D., and Steitz, J. A. (1991) An intact Box C sequence in the U3 snRNA is required for binding of fibrillarin, the protein common to the major family of nucleolar snRNPs. *EMBO J.* **10,** 2645–2651
32. Aris, J. P., and Blobel, G. (1991) cDNA cloning and sequencing of human fibrillarin, a conserved nucleolar protein recognized by autoimmune antisera. *Proc. Natl. Acad. Sci. U.S.A.* **88,** 931–935
33. Horsey, E. W., Jakovljevic, J., Miles, T. D., Harnpicharnchai, P., and Woolford, J. L., Jr. (2004) Role of the yeast Rrp1 protein in the dynamics of preribosome maturation. *RNA* **10,** 813–827
34. Savino, T. M., Bastos, R., Jansen, E., and Hernandez-Verdun, D. (1999) The nucleolar antigen Nop52p, the human homologue of the yeast ribosomal RNA processing RRP1, is recruited at late stages of nucleogenesis. *J. Cell Sci.* **112,** 1889–1900
35. Savino, T. M., Gébrane-Younès, J., De Mey, J., Sibarita, J. B., and Hernandez-Verdun, D. (2001) Nucleolar Assembly of the rRNA Processing Machinery in Living Cells. *J. Cell Biol.* **153,** 1097–1110
36. Yanagida, M., Shimamoto, A., Nishikawa, K., Furuichi, Y., Isobe, T., and Takahashi, N. (2001) Isolation and proteomic characterization of the major proteins of the nucleolin-associating ribonucleoprotein complexes. *Proteomics* **1,** 1390–1404
37. Stavreva, D. A., Kawasaki, M., Dundr, M., Koberna, K., Müller, W. G., Tsujimura-Takahashi, T., Komatsu, W., Hayano, T., Isobe, T., Raska, I., Misteli, T., Takahashi, N., and McNally, J. G. (2006) Potential roles for ubiquitin and the proteasome during ribosome biogenesis. *Mol. Cell. Biol.* **26,** 5131–5145
38. Watkins, N. J., Lemm, I., Ingelfinger, D., Schneider, C., Hossbach, M., Urlaub, H., and Lührmann, R. (2004) Assembly and maturation of the U3 snoRNP in the nucleoplasm in a large dynamic multiprotein complex. *Mol. Cell* **16,** 789–798
39. Fujiyama-Nakamura, S., Yoshikawa, H., Homma, K., Hayano, T., Tsujimura-Takahashi, T., Izumikawa, K., Ishikawa, H., Miyazawa, N., Yanagida, M., Miura, M., Shinkawa, T., Yamauchi, Y., Isobe, T., and Takahashi, N. (2009) Parvulin (Par14), a peptidyl prolyl *cis-trans* isomerase, is a novel rRNA-processing factor that evolved in the metazoan lineage. *Mol. Cell. Proteomics* **8,** 1552–1565
40. Hayano, T., Yanagida, M., Yamauchi, Y., Shinkawa, T., Isobe, T., and Takahashi, N. (2003) Proteomic analysis of human Nop56p-associated preribosomal ribonucleoprotein complexes: Possible link between Nop56p and the nucleolar protein treacle responsible for Treacher Collins syndrome. *J. Biol. Chem.* **278,** 34309–34319
41. Pestov, D. G., Lapik, Y. R., and Lau, L. F. (2008) Assays for ribosomal RNA processing and ribosome assembly. *Curr. Protoc. Cell Biol.* **22,** Unit 22.11
42. Takahashi, N., and Isobe, T. in Proteomic Biology using LC/MS, Wiley Interscience, John Wiley and Sons Inc., Hoboken NJ U.S.A. (2007) pp. 1–254
43. Even, Y., Durieux, S., Escande, M. L., Lozano, J. C., Peaucellier, G., Weil, D., and Geneviève, A. M. (2006) CDC2L5, a Cdk-like kinase with RS domain, interacts with the ASF/SF2-associated protein p32 and affects splicing in vivo, *J. Cell. Biochem.* **99,** 890–904
44. Crawford, N. P., Yang, H., Mattaini, K. R., and Hunter, K. W. (2009) The metastasis efficiency modifier ribosomal RNA processing 1 homolog B (RRP1B) is a chromatin-associated factor. *J. Biol. Chem.* **284,** 28660–28673
45. Tycowski, K. T., Smith, C. M., Shu, M. D., and Steitz, J. A. (1996) A small nucleolar RNA requirement for site-specific ribose methylation of rRNA in *Xenopus. Proc. Natl. Acad. Sci. U.S.A.* **93,** 14480–14485
46. Jansen, R. P., Hurt, E. C., Kern, H., Lehtonen, H., Carmo-Fonseca, M., Lapeyre, B., and Tollervey, D. (1991) Evolutionary conservation of the human nucleolar protein fibrillarin and its functional expression in yeast. *J. Cell Biol.* **113,** 715–729
47. Turner, A. J., Knox, A. A., Prieto, J. L., McStay, B., and Watkins, N. J. (2009) A novel small-subunit processome assembly intermediate that contains the U3 snoRNP, nucleolin, RRP5, and DBP4. *Mol. Cell. Biol.* **29,** 3007–3017
48. Granneman, S., Vogelzangs, J., Lührmann, R., van Venrooij, W. J., Pruijn, G. J., and Watkins, N. J. (2004) Role of pre-rRNA base pairing and 80S complex formation in subnucleolar localization of the U3 snoRNP. *Mol. Cell. Biol.* **24,** 8600–8610
49. Ginisty, H., Amalric, F., and Bouvet, P. (1998) NCL functions in the first step of ribosomal RNA processing. *EMBO J.* **17,** 1476–1486
50. Henning, D., So, R. B., Jin, R., Lau, L. F., and Valdez, B. C. (2003) Silencing of RNA helicase II/Guα inhibits mammalian ribosomal RNA production. *J. Biol. Chem.* **278,** 52307–52314
51. Castle, C. D., Cassimere, E. K., Lee, J., and Denicourt, C. (2010) Las1L is a nucleolar protein required for cell proliferation and ribosome biogenesis. *Mol. Cell. Biol.* **30,** 4404–4414
52. Srivastava, L., Lapik, Y. R., Wang, M., and Pestov, D. G. (2010) Mammalian DEAD box protein Ddx51 acts in 3′ End maturation of 28S rRNA by promoting the release of U8 snoRNA. *Mol. Cell. Biol.* **30,** 2947–2956
53. Eilbracht, J., Reichenzeller, M., Hergt, M., Schnölzer, M., Heid, H., Stöhr, M., Franke, W. W., and Schmidt-Zachmann, M. S. (2004) NO66, a highly conserved dual location protein in the nucleolus and in a special type of synchronously replicating chromatin. *Mol. Biol. Cell* **15,** 1816–1832
54. Zirwes, R. F., Eilbracht, J., Kneissel, S., and Schmidt-Zachmann, M. S. (2000) A novel helicase-type protein in the nucleolus: protein NOH61. *Mol. Biol. Cell* **11,** 1153–1167
55. Heindl, K., and Martinez, J. (2010) Nol9 is a novel polynucleotide 5′-kinase involved in ribosomal RNA processing. *EMBO J.* **29,** 4161–4171
56. Haindl, M., Harasim, T., Eick, D., and Muller, S. (2008) The nucleolar SUMO-specific protease SENP3 reverses SUMO modification of nucleophosmin and is required for rRNA processing. *EMBO Rep.* **9,** 273–279
57. Finkbeiner, E., Haindl, M., and Muller, S. (2011) The SUMO system controls nucleolar partitioning of a novel mammalian ribosome biogenesis complex. *EMBO J.* **30,** 1067–1078
58. Brokstad, K. A., Kalland, K. H., Russell, W. C., and Matthews, D. A. (2001) Mitochondrial protein p32 can accumulate in the nucleus. *Biochem. Biophys. Res. Comm.* **281,** 1161–1169
59. Izumikawa, K., Yanagida, M., Hayano, T., Tachikawa, H., Komatsu, W., Shimamoto, A., Futami, K., Furuichi, Y., Shinkawa, T., Yamauchi, Y., Isobe, T., and Takahashi, N. (2008) Association of human DNA helicase RecQ5β with RNA polymerase II and its possible role in transcription. *Biochem. J.* **413,** 505–516
60. Fogal, V., Richardson, A. D., Karmali, P. P., Scheffler, I. E., Smith, J. W., and Ruoslahti, E. (2010) Mitochondrial p32 Protein Is a Critical Regulator of Tumor Metabolism via Maintenance of Oxidative Phosphorylation. *Mol. Cell. Biol.* **30,** 1303–1318
61. Takahashi, N., Yanagida, M., Fujiyama, S., Hayano, T., and Isobe, T. (2003) Proteomic snapshot analysis preribosomal ribonucleoprotein complexes formed at various stages of ribosome biogenesis in yeast and mammalian cells. *Mass Spectrom. Rev.* **22,** 287–317
62. Kawasaki, M. (2004) Master's thesis (Isolation and proteomic characterization of the preribosomal ribonucleoprotein complex associated with a novel nucleolar protein-1 that is ubiquitously expressed in human tissue), Graduate School of Agriculture, Tokyo University of Agriculture & Technology
63. Snaar, S., Wiesmeijer, K., Jochemsen, A. G., Tanke, H. J., and Dirks, R. W. (2000) Mutational analysis of fibrillarin and its mobility in living human cells. *J. Cell Biol.* **151,** 653–662
64. Jiang, J., Zhang, Y., Krainer, A. R., and Xu, R. M. (1999) Crystal structure of human p32, a doughnut-shaped acidic mitochondrial matrix protein. *Proc. Natl. Acad. Sci. U.S.A.* **96,** 3572–3577
65. Seytter, T., Lottspeich, F., Neupert, W., and Schwarz, E. (1998) Mam33p, an oligomeric, acidic protein in the mitochondrial matrix of *Saccharomyces cerevisiae* is related to the human complement receptor gC1q-R. *Yeast*

14, 303–310
66. Harnpicharnchai, P., Jakovljevic, J., Horsey, E., Miles, T., Roman, J., Rout, M., Meagher, D., Imai, B., Guo, Y., Brame, C. J., Shabanowitz, J., Hunt, D. F., and Woolford, J. L., Jr. (2001) Composition and functional characterization of yeast 66S ribosome assembly intermediates. *Mol. Cell* **8,** 505–515
67. Ho, Y., Gruhler, A, Heilbut, A., Bader, G. D., Moore, L., Adams, S. L., Millar, A., Taylor, P., Bennett, K., Boutilier, K., Yang, L., Wolting, C., Donaldson, I., Schandorff, S., Shewnarane, J., Vo, M., Taggart, J., Goudreault, M., Muskat, B., Alfarano, C., Dewar, D., Lin, Z., Michalickova, K., Willems, A. R., Sassi, H., Nielsen, P. A., Rasmussen, K. J., Andersen, J. R., Johansen, L. E., Hansen, L. H., Jespersen, H., Podtelejnikov, A., Nielsen, E., Crawford. J., Poulsen, V., Sørensen, B. D., Matthiesen, J., Hendrickson, R. C., Gleeson, F., Pawson, T., Moran, M. F., Durocher, D., Mann, M., Hogue, C. W., Figeys, D., and Tyers, M. (2002) Systematic identification of protein complexes in *Saccharomyces cerevisiae* by mass spectrometry. *Nature* **415,** 180–183
68. Simonin, D., Diaz, J. J., Massé, T., and Madjar, J. J. (1997) Persistence of ribosomal protein synthesis after infection of HeLa cells by herpes simplex virus type 1. *J. Gen. Virol.* **78,** 435–443
69. Besse, S., and Puvion-Dutilleul, F. (1996) Intranuclear retention of ribosomal RNAs in response to herpes simplex virus type 1 infection. *J. Cell Sci.* **109,** 119–129
70. Ponti, D., Troiano, M., Bellenchi, G. C., Battaglia, P. A., and Gigliani, F. (2008) The HIV Tat protein affects processing of ribosomal RNA precursor. *BMC Cell Biol.* **9,** 32
71. Shirai, C., Takai, T., Nariai, M., Horigome, C., and Mizuta, K. (2004) Ebp2p, the yeast homolog of Epstein-Barr virus nuclear antigen 1-binding protein 2, interacts with factors of both the 60 S and the 40 S ribosomal subunit assembly. *J. Biol. Chem.* **279,** 25353–25358
72. Hiscox, J. A. (2002) The nucleolus-a gateway to viral infection? *Arch. Virol.* **14,** 1077–1089
73. Hiscox, J. A. (2007) RNA viruses: hijacking the dynamic nucleolus. *Nat. Rev. Microbiol.* **5,** 119–127
74. Raychaudhuri, S., Fontanes, V., Barat, B., and Dasgupta, A. (2009) Activation of ribosomal RNA transcription by hepatitis C virus involves upstream binding factor phosphorylation via induction of cyclin D1. *Cancer Res.* **69,** 2057–2064
75. Hadjiolova, K. V., Nicoloso, M., Mazan, S., Hadjiolov, A. A., and Bachellerie, J. P. (1993) Alternative pre-rRNA processing pathways in human cells and their alteration by cycloheximide inhibition of protein synthesis. *Eur. J. Biochem.* **212,** 211–215